國立臺灣大學醫學院生物化學暨分子生物學研究所

碩士論文

Graduate Institute of Biochemistry and Molecular Biology

College of Medicine

National Taiwan University

Master Thesis

利用矽奈米線場效應電晶體開發以嗜中性白血球明膠

酶相關運載蛋白為指標的急性腎臟損傷快速診斷晶片

Development of NGAL fast biochip using Silicon
Nanowire Field-Effect Transistors for Acute Kidney Injury
Detection

鄭丞斌

Cheng-Pin Cheng

指導教授：周綠蘋 博士

Advisor: Lu-Ping Chow, Ph.D.

中華民國 107 年 7 月

July 2018

國立臺灣大學碩士學位論文
口試委員會審定書

利用矽奈米線場效應電晶體開發以嗜中性白血球明膠酶相關
運載蛋白為指標的急性腎臟損傷快速診斷晶片
Development of NGAL fast biochip using Silicon Nanowire
Field-Effect Transistors for Acute Kidney Injury Detection

本論文係 鄭丞斌 君（R05442022）在國立臺灣大學生物化學暨
分子生物學研究所、所完成之碩士學位論文，於民國 107 年 7 月 30
日承下列考試委員審查通過及口試及格，特此證明

口試委員：

　　　　　　　　（簽名）
　　　　　　　（指導教授）

系主任、所長　　　　　　　　　（簽名）

謝誌

如果有機會，我會想要繼續延續這份幸運。

當初因為大學四年下來生化學成績最差，所以選擇了生化分生所，因為對於蛋白質領域的不了解，所以到了 周綠蘋老師的實驗室。我並沒有特別想要挑戰什麼，但是至少不想要有某些領域過於薄弱。

結果拿到了一個跨越生化領域及電機領域的題目。

當初知道自己要做的是跨領域時，可能有興奮也可能會怕，但更多的只是單純不知道要怎麼做。我自己在面對問題，都會先找個小的著力點，分析好問題再依照這個遇到的問題解決，但是關於半導體的一切我卻不知道該怎麼做。沒有讀電機的朋友，大學沒有學過半點物理，甚至高中的時候物理也是最頭痛的科目之一。我找了電子書，找朋友拿講義，找朋友的朋友問了一些相關的事情，但沒有任何幫助，說實在的連要看什麼、要查什麼都沒有半點頭緒。第一個得要感謝帶我入門的悅筑學姊，她從最簡單的 ELISA 帶我做起，不管當初那 standard curve 上面的點如何頑皮地散落，她都不會露出半點無奈、不想帶我的感覺，學姊教我細膩讓我逐漸度過卡關的每個實驗，也讓我有了這個題目所具備的基礎。接下來要感謝像越過多個山丘才努力畢業的裕凱學長。因為換題目以及畢業的壓力，學長搶在我的前面完成了超多實驗，不管是純化蛋白、ELISA 建立、各種 stripping buffer 測試，雖然後來很可惜沒有完成，但在晶片實驗上仍然留下了很多有用的參考。另外感謝實驗室很可愛的學弟妹，學長姊，還有平常沒事就吃飯聊實驗的同學們，平凡的實驗室生活中，如果沒有常常聚在一起聊天玩樂，那麼兩年的日子不會這麼開心地飛逝，可以在兩年之中認識這麼多以後可能會共同打拼的同伴們，算是相當值得相當划算的兩年！

接下來要感謝 周綠蘋老師，現在回想當初接下這個題目，有點不可思議，像是走過根本沒有道路指引的森林。與其說克服了哪些困難，我真正感動的是老師幾

i

乎是放手讓我去嘗試了很多不同的東西，兩年下來沒有被老師罵過什麼，還能常常輕鬆地聊天，我不知道算不算難能可貴，但是可以沒有壓力的討論實驗，面對不同問題，一項一項慢慢往前推進，是非常幸福的碩班生涯！再來要感謝提供檢體的吳醫師和當初給我重大建議的 林致廷老師，每次去找 林老師討論實驗，或許時間都不長，但短時間都能學到非常多沒有想到的觀點或很有用的實驗邏輯，也因為這些討論，能讓我順利的畢業。同時也要感謝聖燁、又豪兩位學長，還有曉蓁及雅晴，麥伯森提供了我非常多晶片和實驗器材，甚至常常都是把量測的時間讓給我使用，如果沒有這些，恐怕這篇碩士論文也無法順利完成。

最後要感謝皮卡丘、阿狐、卓然、居安、家人、還有碩班期間的同學，芃瑞、靜瑩、家君芷嫻二人組、宇軒、予晨，還有球隊認識的好朋友們(Ex.書發)，神奇的學長黃韜，超強的星星大神仲豪，陪我打球的偉程欣郁二人組，人總是很好的品欣、沛樺、家齊，還有每次都願意聽我講很多很多話的雅惠，我是很任性自私的小孩，不想長大也不想妥協於這個社會的一分一毫，只想聽到皮卡丘很可愛、只想聽到有人聽我講解天空的星星，只想嚴肅且溫柔地挑戰這個社會持續的不公平，當然有人對我充滿歧見，但更多的是我感受到大家對我過分的好，並且願意幫助或支持我、甚至願意不斷給我掌聲。感謝一路上曾經打鬧談心的人們，許多我的故事都是由你們一起寫的，希望哪天有人再次翻開這本論文，能知道是因為大家的支持，才得以完成這篇論文。

摘要

急性腎臟損傷(acute kidney injury, AKI)是腎臟功能快速下降或損壞。一般來說，急性腎臟損傷的死亡率大約在20%。用來診斷急性腎臟損傷主要是依據血清肌酸酐和排尿量來做為診斷依據，然而，這兩個指標在診斷急性腎臟損傷都不夠快速。血清肌酸酐會在AKI之後一到三天上升，根據估計，在血清肌酸酐上升前，超過50%的腎臟功能已經喪失。因此，血清肌肝酸並不能在急性期正確的反應腎絲球過濾率的下降情形。另一方面，一些生物指標像是嗜中性白血球明膠酶相關運載蛋白(neutrophil gelatinase-association lipocalin, NGAL)或乾脂肪酸結合蛋白會在急性期早期上升。一般來說，NGAL用來預測AKI的曲線下的平均面積(area under the receiver-operating characteristic curve , AUC-ROC)是0.79，同時NGAL會在手術後四小時內上升並達到最高峰。傳統的酵素免疫分析法非常耗時，因此，為了要更快速即時有效的偵測急性腎臟損傷，我們想要利用矽奈米線場效應電晶體(Silicon nanowire-field effect transistor, SiNW-FET)發展一個能將偵測時間縮小到30以內的快速診斷晶片。

在本篇的研究中。我們首先成功的純化NGAL重組蛋白，並且成功地建立可以被用來當作標準對照方法的酵素免疫分析法。接著我們決定了抗體固著的步驟，並且發現了在羥化過程中，在過氧化氫、膽酸、氫氧化鈉裡面，膽酸在r平方和飄移速度的表現是三者最佳。在矽烷化過程中，我們發現比起過去常用的APTES，AEAPTES比較不會進行自我反應。藉由觀察及量測FET生物晶片的電流變化，我們就能在30分鐘之內知道蛋白質的含量。在本篇的研究中，7個AKI和5個非AKI檢體被定量，利用這個SiNW-FET系統定量的AKI檢體所測量出的NGAL範圍為1500到4000 ng/mL，同時4個非AKI檢體的NGAL量測出來是0 ng/mL。藉由使用SiNW-FET系統，AKI和非AKI檢體可以顯著地被區分開來(p value小於0.001)。總結本篇論文，我們開發了快速偵測晶片，可以用來臨床的定量，並且可以用來分開AKI和

非AKI兩個族群。

Abstract

Acute kidney injury (AKI) is condition of rapid or abrupt decline in renal function. Overall, the mortality of AKI is 20%. Serum creatinine and urine output are used to define the prognosis of AKI. However, both indicators are not fast enough to detect AKI. Increase of serum creatinine occurred within 1 to 3 days after AKI; and it is estimated that greater than 50% of kidney function must be lost before serum creatinine rises. Consequently, serum creatinine does not reflect the true decrease of glomerular filtration rate in the acute setting. On the other hand, indicators such as neutrophil gelatinase-associated lipocalin (NGAL) and liver-type fatty acid binding protein increased at an early stage. Generally, the avera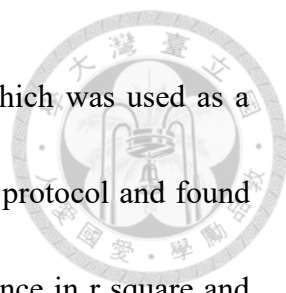ge area under the receiver-operating characteristic curve (AUC-ROC) of predicting AKI by NGAL was 0.79; and NGAL level arises and achieves their peak level arises within four hours after surgeries[1]. Conventional enzyme-linked immunosorbent assay (ELISA) is time-consuming. In order to perform real-time detection of AKI, we developed a fast-detecting biochip using silicon nanowire field-effect transistor (SiNW FET) which can reduce the detection time to less than 30 minutes.

In this study, we first successfully purified NGAL recombinant protein and well established NGAL ELISA, which was used as a standard method to compare with. Next, we determined the coating protocol and fIn this study, we first successfully purified

NGAL recombinant protein and well established NGAL ELISA, which was used as a standard method to compare with. Next, we determined the coating protocol and found that in the hydroxylation process, cholic acid had the best performance in r square and drifting rate among H_2O_2, cholic acid and NaOH. In the silanization process, we found that AEAPTES was less prone to self-react than APTES, which was commonly used beforeound that in the hydroxylation process, cholic acid had the best performance in r square and drifting rate among H_2O_2, cholic acid and NaOH. In the silanization process, we found that AEAPTES was less prone to self-react than APTES, which was commonly used before. By observing and measuring the current change, we could know the protein level within 30 minutes. In this study, 7 AKI and 5 non-AKI samples were quantified. NGAL levels of AKI patients quantified by this system ranged from 1500 to 4000 ng/mL, while levels of four non-AKI samples were 0 ng/mL. By using the SiNW-FET system, AKI and non-AKI samples can be discriminated significantly (p value<0.001). In conclusion, we developed a fast detecting biochip that can be applied to clinical quantification which is able to discriminate AKI and non-AKI samples.

CONTENTS

LIST OF TABLES AND FIGURES

Chapter 1.   Introduction

1.1   Acute kidney injury

Acute Kidney Injury (AKI) is a common condition seen in acutely ill patients,

which results in rapid loss of kidney functions within hours to days[2]. The major

characteristic of AKI is reduction in renal excretory function. Without efficient excretion,

nitrogen metabolites, including urea and creatinine, accumulate in blood and deal damage

the kidney and renal tubules. According to their causes, AKI is classified into three groups,

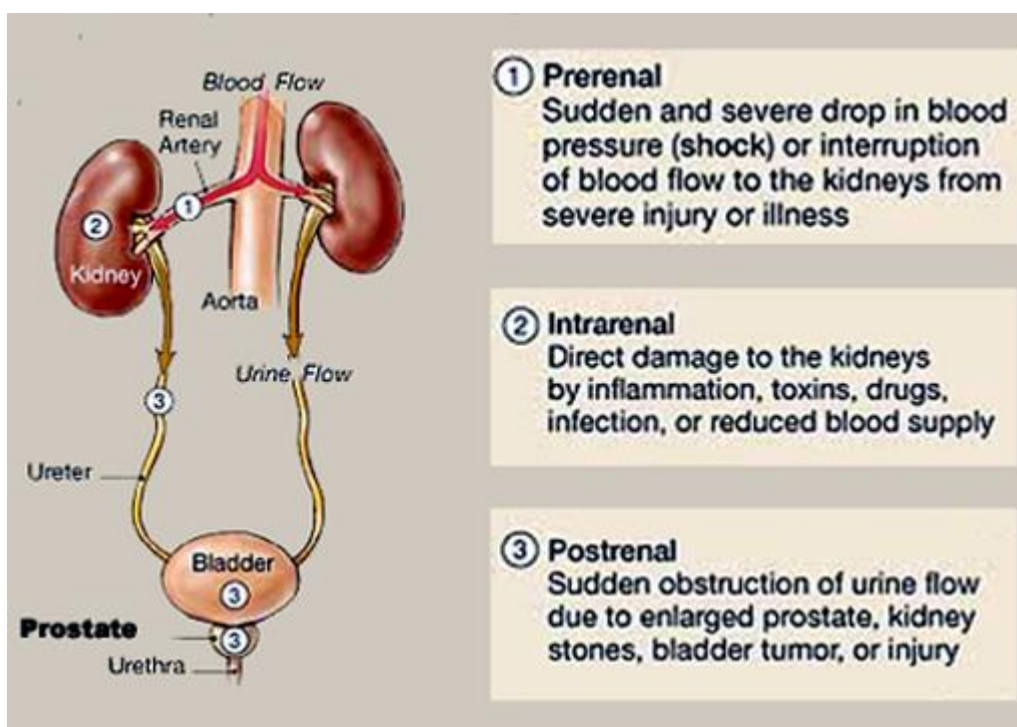prerenal, intrarenal, and postrenal AKI (figure 1).

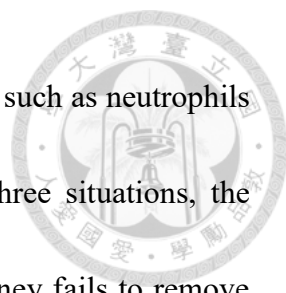Figure 1 Acute kidney injury and the three subtypes[3].

1.1.1   Prerenal AKI

In prerenal AKI, decreased excretory function is mainly due to decreased blood flow[4]. In normal situation, blood is filtered through glomerulus and form filtrate. When blood supply decrease, glomerular filtration rate (GFR) decrease and unable to remove nitrogen wastes. The causes of prerenal AKI vary widely, from simple embolus in renal artery, major hemorrhage, renal artery stenosis, vomiting, to cardiovascular surgery-induced hypotension.

1.1.2   Intrarenal AKI

In intrarenal AKI, the glomerulus, the renal tubules, or interstitium are directly damaged and therefore unable to carry out normal renal functions[5]. There are several possibilities to induce direct renal damages, including vasculitis, infection, sepsis, toxin or developer intake, and glomerulonephritis. Briefly, intrarenal AKI can be classified into three classes, glomerulonephritis, acute tubular necrosis, and acute interstitial nephritis. In glomerulonephritis, since blood is filtered through glomerulus with the help of pressure difference, once the glomerulus is damaged, the pressure difference reduces and the GFR will become lower. In acute tubular necrosis, the renal tubular cells are dead that cause the kidney cannot perform reabsorption and secretion which results in low GFR. In acute

2

interstitial nephritis, renal interstitium is infiltrated by immune cells, such as neutrophils and eosinophils, that initiates inflammatory responds. In all the three situations, the kidney fails to filter, reabsorption, and secretion. Therefore, the kidney fails to remove nitrogen wastes.

1.1.3 Postrenal AKI

In postrenal AKI, ureter or urinary tract is blocked or obstructed. The obstruction or the blockage will result in high pressure within the ureter[6]. In normal situation, ureter is under low pressure while the glomerulus is in high pressure. When pressure in ureter increases, pressure difference become lower and therefore reduce the GFR. In general, any types of obstruction may cause postrenal AKI, such as benign prostate hyperplasia, kidney stone, bladder stone, or even tumors[7]. The treatment of postrenal AKI is to remove these blockages, rebuilding the pressure difference between glomerulus and ureter.

1.2 Staging and Prognosis

The RIFLE classification was proposed in May 2004 as a AKI staging criteria[8]. The RIFLE refers to risk, injury, failure, loss, and end-stage kidney disease
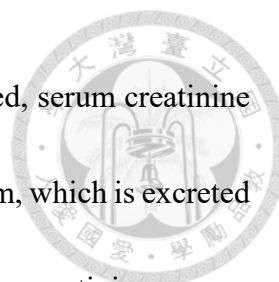
(Figure 2). In the RIFLE classification system, two indicators are used, serum creatinine and urine output (UO). Creatinine is a byproduct of muscle metabolism, which is excreted by kidney. Once the kidney is damaged and fail to remove serum creatinine, serum creatinine level increased. The other indicator, urine output, represents the urine-producing ability of kidneys. Therefore, combination of these indicators could clearly reflect the kidney function.
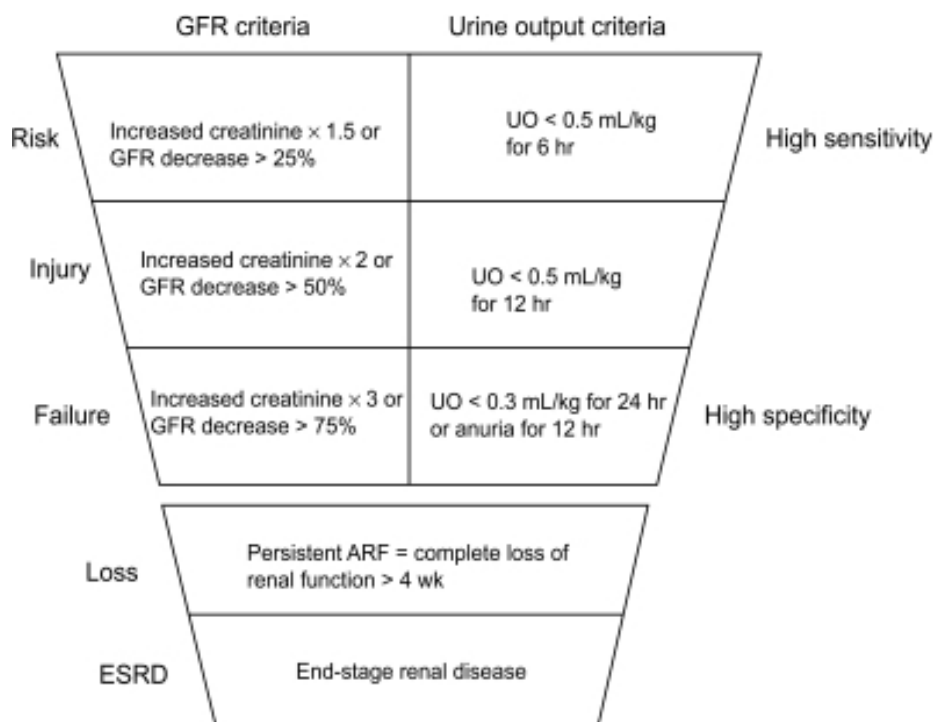

Figure 2 RIFLE acute kidney injury classification[9].

Typically, prognosis of AKI could be divided into four phases, onset phase, oliguric/anuric phase, diuretic phase, and recovery phase (table 1)[10]. In the beginning of onset phase, the kidney function starts to decline within hours to days. Both urine output and blood supply decrease in this phase. If not treated, it will enter oliguric/anuric

4
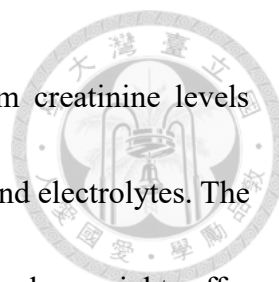
phase. In the oliguric/anuric phase, blood urea nitrogen and serum creatinine levels increase and the kidney is unable to remove unwanted or excess H^+ and electrolytes. The oliguric/anuric could last for weeks or even longer and patients in this phase might suffer from acidosis and need hemodialysis or renal replacement therapy. If the AKI patients receive proper treatment, it will enter diuretic phase and recovery phase and restore kidney function.

Four phases of AKI

This chart describes the features and durations of the four phases of acute kidney injury (AKI).

Phase	Features	Duration
Onset phase	• Common triggering events: significant blood loss, burns, fluid loss, diabetes insipidus • Renal blood flow 25% of normal • Tissue oxygenation 25% of normal • Urine output below 0.5 mL/kg/hour	Hours to days
Oliguric (anuric) phase	• Urine output below 400 mL/day, possibly as low as 100 mL/day • Increases in blood urea nitrogen (BUN) and creatinine levels • Electrolyte disturbances, acidosis, and fluid overload (from kidney's inability to excrete water)	8 to 14 days or longer, depending on nature of AKI and dialysis initiation
Diuretic phase	• Occurs when cause of AKI is corrected • Renal tubule scarring and edema • Increased glomerular filtration rate (GFR) • Daily urine output above 400 mL • Possible electrolyte depletion from excretion of more water and osmotic effects of high BUN	7 to 14 days
Recovery phase	• Decreased edema • Normalization of fluid and electrolyte balance • Return of GFR to 70% or 80% of normal	Several months to 1 year

Table 1. Four phases of AKI[10].

1.3 Novel Biomarkers

In the RIFLE classification, serum creatinine and urine output is used as AKI staging indicators. However, according to a study of 2010[1], more than 50% of kidney function has been lost before serum creatinine arise (figure 3). Therefore, we need more reliable biomarkers that could represent the true damage situation. Previous studies have shown that new biomarkers, such as neutrophil gelatinase-associated lipocalin (NGAL), liver type fatty-acid-binding protein (L-FABP), kidney injury molecule-1, and interleukin 18, arise at early stage of kidney injury (figure 4)[1, 11-13]. When renal cells are exposed to pressure condition, such as ischemia-reperfusion or toxicity, these novel biomarkers are released in response to the damage before necrosis and cell death. Some of these biomarkers have protective effect. For example, L-FABP were reported to be a reactive oxygen species cleaner while NGAL could alleviate the progress and deterioration of mice AKI[12, 14]. Therefore, early detection of these novel biomarkers are helpful for early detection of AKI and could provide patients better prognosis.
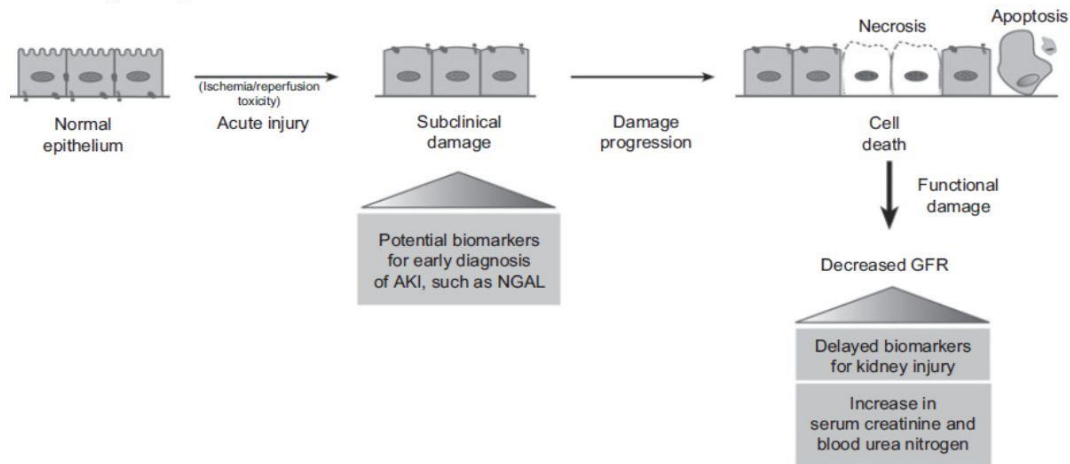
Figure 3 The progression of acute kidney injury[15]
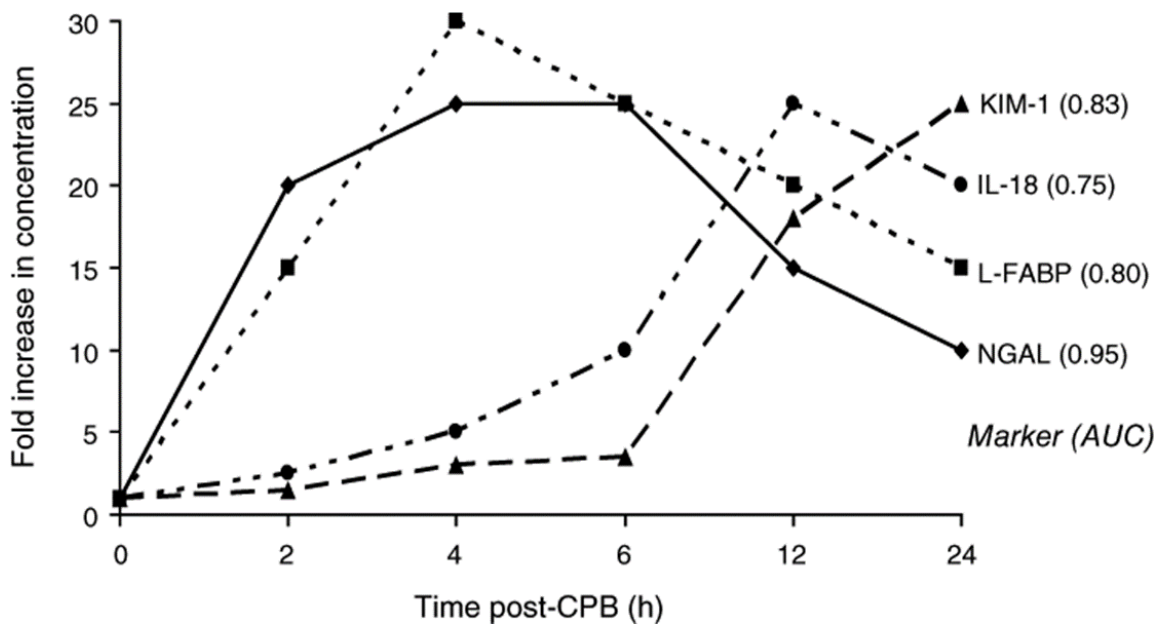

Figure 4 Novel biomarkers increase at early stage of acute kidney injury[1]

1.4   Neutrophil gelatinase-association lipocalin

Neutrophil gelatinase-association lipocalin (NGAL), as its name implies, is originally found in neutrophil which function as an iron and siderophore shuttle (figure 4)[16]. NGAL belongs to lipocalin family and is encoded by *LCN2*. Members of lipocalin family have a single eight-stranded anti-parallel b-barrel which forms a space that enable transportation of small hydrophobic molecules. Because of this unique structure, lipocalins could act as a transporter or a shuttle for many different molecules, such as retinoids, arachidonic acid, prostaglandins, fatty acids, pheromones, steroids, and iron[17]. NGAL is composed of 178 amino acids and is about 25 kD, which have high affinity with iron-containing siderophore[18]. Bacteria produce siderophore to transport extracellular iron into intracellular space, indicating bacteria need iron for cell growth. When facing bacterial infection, neutrophil releases NGAL to sequester iron-containing siderophore and thereby inhibit bacterial growth[16].
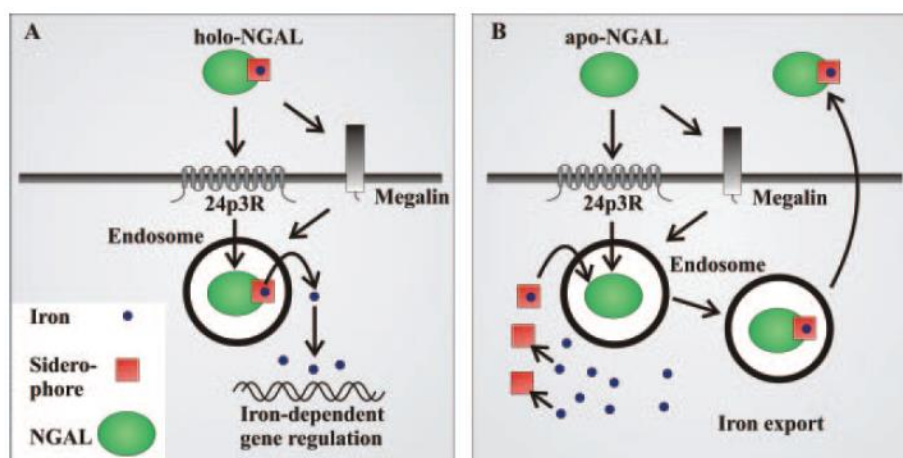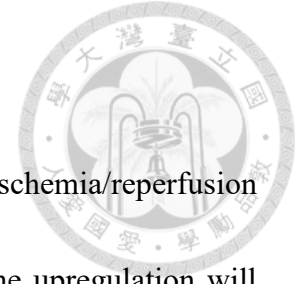

Figure 5 Neutrophil gelatinase-association lipocalin is an iron and siderophore shuttle[16]

8

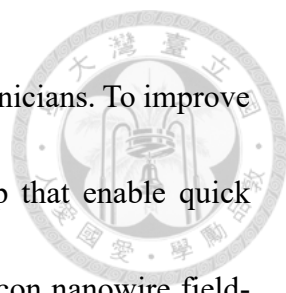## 1.5 NGAL in acute kidney injury

According to previous study, they found that under renal ischemia/reperfusion condition, transcription of *Lcn2* was upregulated in 3 hours and the upregulation will persist for 2 days[19]. Likely, according to a group from National Institute of Diabetes and Digestive and Kidney Diseases, Maryland, they used microarray to compare the transcriptome between pre- and post-AKI[20]. They also found Lcn2 was upregulated after renal ischemia/reperfusion or $HgCl_2$-induced AKI. At the level of protein, NGAL was identified as an upregulated protein after acute renal damage[20]. In acute renal failure mice, NGAL mRNA had a 3-fold increase within one hour while protein had a 2-fold increase within 2 hours. In 2004, they also proved similar results in kidney biopsy of cisplatin-induced AKI. In clinical research, by using ELISA, they found that urinary NGAL had a 10-fold increase within 2 to 6 hours in children who receive cardiac surgery and develop AKI[15]. The AUC-ROC was greater than 0.9. Other clinical data also confirmed the elevation of NGAL in adult patients who receiving cardiac surgery and develop AKI within 2 to 6 hours. The AUC-ROC ranges from 0.61 to 0.96. The possible reasons for the low AUC-ROC includes chronic kidney disease, other chronic illness, or diabetes. Since NGAL can be secreted by neutrophil, these chronic diseases might slightly influence sensitivity and specificity of the biomarker[15]. Taken together, all of these researches showed strong evidences that NGAL is highly induced in early onset of acute

9

kidney injury and could be used as a biomarker for AKI.

Biologically, release of NGAL is a protective mechanism against ischemic acute renal injury. According to a study of 2004, (JAYA MISHRA et. Al, 2004, Amelioration of Ischemic Acute Renal Injury by Neutrophil Gelatinase–Associated Lipocalin), they found intravenous injection of NGAL ameliorated the damage from ischemic AKI[14]. Murine kidneys pre-treated with NGAL displayed better histopathological response, including fewer cast production, attenuated cell necrosis, and better tubule dilatation score. In addition, NGAL improved proliferation of renal tubular cell after ischemic damage. By calculating the ratio between cell survival and cell death, they observed that pre-treating NGAL increase the ratio of proliferation versus necrosis and apoptosis. Despite the detailed mechanism of NGAL remains unknown, NGAL could attenuated histopathological damage by ischemic AKI.

1.6   Silicon Nanowire Field-Effect Transistor (SiNW-FET) Biochip

Because of the limitation of traditional biomarkers and time-consuming methodologies, it is still difficult to detect AKI within several hours. Therefore, it's necessary to develop new techniques to achieve fastness and reliability. Unlike many newly developed label-free techniques, traditional enzyme-linked immunosorbent assay

(ELISA) is a time-consuming and is heavily rely on experienced technicians. To improve the disadvantages, we would like to develop fast-detecting biochip that enable quick semi-quantification and discriminate AKI and non-AKI groups. Silicon nanowire field-effect transistor is a semiconductor-based technique, which can sense the electric field of the analyte. This technique was developed and used in pH sensing and ion detecting for over fifteen years. It is characterized by its small size, high sensitivity, label-free and real-time detection[21]. Moreover, SiNW-FET can be applied to detection of a wide range of biomolecules, such as hepatitis B viral DNA, prostate specific antigen, and troponin[22-26]. In general, SiNW-FET biochip is designed as figure 6a. The silicon dioxide is the layer that contact to the bio-molecules and the semi-conductor underneath the silicon dioxide layer is connect to a wire for current measurement. The semi-conductor of the chip is able to sense the electric field of the protein or DNA molecules outside the silicon dioxide, and results in current change detected by the wire. In practice, antibodies will be fixed on the silicon dioxide, and capture antigen in the sample. When analyte in the sample was captured by the antibody, sensor underneath the silicon dioxide can sense the current change. More specifically, take N-type semiconductor-based SiNW-FET and positive-charged molecules for example, when positive-charged analytes are captured by antibody, electrons within the N-type semiconductor will move forward to the side of the analytes. The accumulation of the electrons obstructs the path of the current, namely,

11
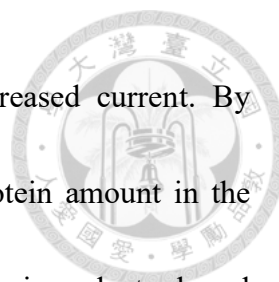
enhances the resistance of the semiconductor and results in decreased current. By

calculating the degree of current decrease, we could know the protein amount in the

sample. Compared to ELISA, because SiNW-FET is label-free and semi-conductor based

assay, the total reaction time of the SiNW-FET can be shortened from more than 5 hours

to less than one hour. Consequently, by using SiNW-FET combined with novel biomarker,

NGAL, it would be a new diagnostic tool to detect AKI faster and provides AKI patients

better prognosis.
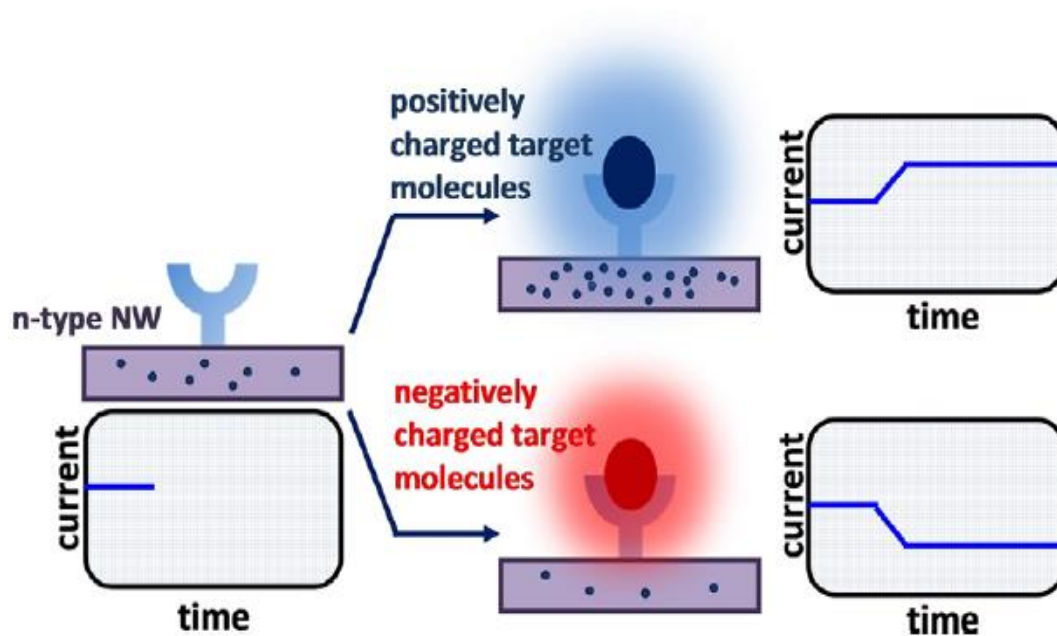
Figure 6 The principle of SiNW-FET biochip

1.7　Specific aim

As mentioned before, traditional indicators, serum creatinine and urine output,

are late indicators for acute kidney injury. In addition, ELISA is a time-consuming

technique and should be performed by well-trained technician. Therefore, with the help of SiNW-FET based platform, we would like to develop a fast-detection assay to detect the progression of acute kidney injury.
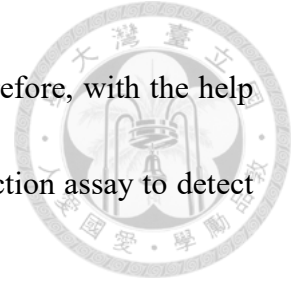
Chapter 2.   Materials and Methods

2.1   Recombinant protein expression and purification

Plasmid pET-28a with human LCN2 gene and two histidine tage was provided by the BioMed Resource Core of the 1st Core Facility Lab, NTU-CM. The vector was transformed into *Escherichia coli* BL21 by 37℃ heat shock and evenly spread on LB plate which contained 1 ng/mL kanamycin. After 12 to 16 hours' incubation at 37℃, single colony was selected and inoculated to 5 mL LB containing 1 ng/mL kanamycin. After incubating 12 to 16 hours at 37℃, the 5 mL LB was transferred to 500 mL LB with 1 ng/mL kanamycin. When the OD$_{600nm}$ reached around 0.75, 1 mM Isopropyl β-D-1-thiogalactopyranoside (IPTG, Sigma) was added to induce protein expression. After 4 hour-induction, the bacteria was centrifugated 6500 rpm for 20 minutes and the pellet was collected. The collected pellet was dissolved in binding buffer (25mM Tris-HCl, 0.5M NaCl, pH8.0) and sonicated. After centrifugation (13500 rpm, 20 minutes), supernatant was collected and purified on a Ni^{2+}-chelating Sepharose column. The induction and elution results were shown on SDS-PAGE and stained with Coomassie blue. The concentration of the purified protein was determined by Pierce BCA protein assay kit.
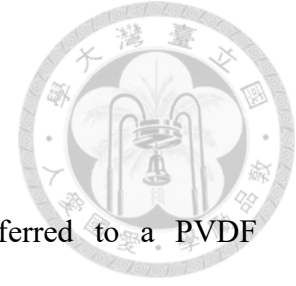
2.2　Immunoblotting analysis

Purified protein performed by SDS-PAGE was transferred to a PVDF membrane (GE healthcare), which was then blocked with blocking buffer (10% nonfat milk in 50 mM Tris-HCL, 150 mM NaCl, pH 7.5). After blocking, the membrane was incubated with anti-His antibody (1:5000) which was diluted in blocking buffer, at 4°C for overnight. After washed, the membrane was incubated with secondary antibody (1:20000) and detected using ECL reaction solution (GE) and visualizing with LAS4000 Luminescent Image Analyzer (Fujifilm).

2.3　Protein identification by LC-MS/MS

2.3.1　In-gel digestion

Having finished SDS-PAGE and CBB staining, cut the target band into pieces of 1 mm^3 and put the gel into eppendorf. Before de-staining the gel, the gel was cleaned by ddH$_2$O thrice. After cleaning, 1 mL of destain buffer (40% acetonitrile, 25 mM NH$_4$HCO$_3$, pH 7.8) was used at 37°C for 30 minutes. After the gel became colorless, 200 μL 100% acetonitrile (ACN) was added to remove the remaining destain buffer and followed by vortex and centrifugation. Repeat the step for two times and the gel would become small and white granules. Next, the gel was hydrolyzed by trypsin, which was

dissolved by 25 mM NH$_4$HCO$_3$ (pH 7.8), at 4°C for 30 minutes until the trypsin was absorbed completely by the gel and followed by 16 hours-incubation at 37°C.
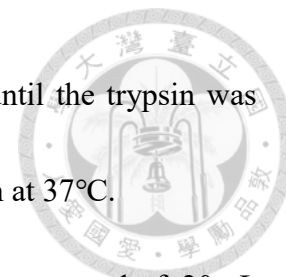
After the incubation, the trypsin buffer was collected to a new eppedorf. 20 μL 1% trifluoroacetic acid (TFA) was added to the origin eppendorf and incubated at 37°C in the ultrasonic waterbath for 30 minutes. After the incubation, the extract was collected and 20 μL 0.1% TFA and 60% ACN was added and incubated at 37°C in the ultrasonic waterbath for 30 minutes. All the extracts were collected in one eppendorf and dried with Speed Vac. If salt was not completely removed, 20 μL 1% formic acid (FA) was used to remove the remaining salt and then dried with Speed Vac.

After drying, 10 μL solution (2% ACN, 0.1% FA) was used to dissolve the peptide. Before adsorbing the peptide to the Supel-tip C18 (Sigma), the tip was activated by 90% activation solution (90% ACN, 0.1% FA) through pipetting 10 times. After discarding the activation solution, the tip was hydrolyzed by balancing solution (2% ACN, 0.1% FA). After discarding the solution, the peptides were adsorbed to the C18 through pipetting the peptide-containing solution for 10 times. Next, washing solution (5% ACN, 0.1% FA) was used and pipetted to remove unbound salt. After that, elution solution (60% ACN, 0.1% FA) was used and pipetted to elute the peptide. The elution solution was collected in a new eppendorf and dried with Speed Vac.

2.3.2　LC-MS/MS analysis

After de-salting and drying, the peptide was dissolved in 2% ACN and 0.1% FA. The peptide was separated through reverse-phase chromatography. After ionizing the peptide by electron spray ionization (ESI), the peptide was selected and sequenced by the mass spectrometry (MS).

2.3.3　Bioinformatics-Mascot Daemon

According to Matrix Science corporation, the identification of peptide was carried out by comparison between the database and MS data. The parameters used in this study is showed in table 1.

Table 1

Protein database	Swiss-Prot
Enzyme name	Trypsin
Max. missed cleavage	1
Taxonomy	Homo sapiens (human)
Variable modifications	Carbamidomethylation
	Deamidated
	Oxidation

	Phosphorylation
Peptide charge	2+, 3+, and 4+
Peptide tol.	± 2 Da
MS/MS tol.	± 0.5 Da

2.4 Quantification of NGAL of AKI and non-AKI patients' urine by ELISA

A total of 253 AKI patients and 20 non-AKI patients were analyzed by sandwich enzyme-linked immunosorbent assay (ELISA). First, 96-well microplates were pre-coated with NGAL capture antibody (R&D) at 4℃ for 12 to 16 hours. After washing away the unbound antibodies, the wells were blocked with 1% bovine serum albumin at room temperature for 1 hour and followed by phosphate-buffered saline with 0.05% tween 20 (PBST) wash. Next, urine samples and recombinant proteins (100 μL) were added and incubated at 37℃ for 2 hours. After washing away the unbound, biotinylated NGAL detection antibody was added and incubated at room temperature for 2 hours. After washing away the unbound antibodies, streptavidin-horse peroxidase (1:200) was added for 1 hour at room tempearture. After washing away the unbound, NeA-Blue (tetramethylbenzidine substrate, R&D) solution was added and the substrates were

18
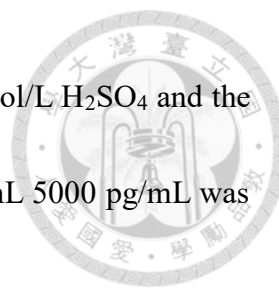
converted to detectable form. Next, the reaction was stopped by 1 mol/L H_2SO_4 and the absorbance was read at 450 nm. A standard curve from 78.125 pg/mL 5000 pg/mL was generated for the assay.

2.5   Design of Si-NW Based Biosensor

Wafer bought from TSC was fabricated by Nuvoton. The design and etching process were shown in figure 2-a. The FET biochip is mainly composed of two poly-Si layer which are covered by silicon dioxide (SiO_2) and two metal layers. In order to achieve better sensitivity, etching process was performed to obtain thinner and proper thickness of SiO_2. Antibody will be fixed onto the etched SiO_2 layer through surface functionalization process. The final thickness of etched SiO_2 is 24 nm. The poly-Si layers are the p-type sensing region, of which the resistance will be altered by the electric field of the proteins. The current of the poly-Si is measured by a single wire, which pass through the metal layer and connect to KEITHLEY 6485 picoammeter.
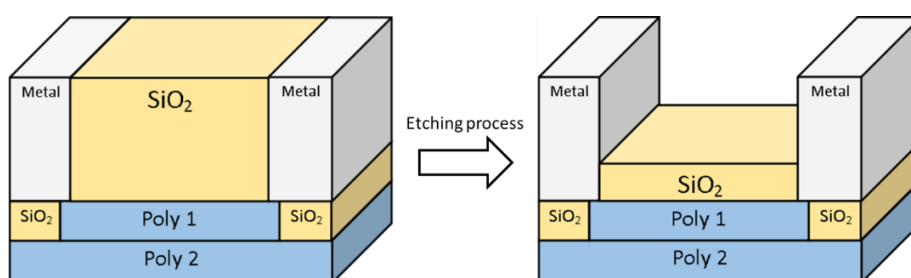
Figure 1 The design and etching process of the SiNW biochip.

19

2.6   Surface modification and functionalization

To functionalize the surface of the Si-NW biochip, the APTES-Glutaraldehyde system was used to immobilize the antibody. There were four major steps, hydroxylation, silanization, formation of glutaraldehyde linkage, and fixation of antibody. First, the chips were immersed in 2% cholic acid dissolved in 95% ethanol at 60°C for 2 hours to generate hydroxyl group on the surface of silicon dioxide and followed by ethanol wash. Next, 2% N-(2-aminoethyl)-3-aminopropyltriethoxysilane (AEAPTES) and was introduced for 1 hour at room temperature with electrical field to attach the silane groups to the hydroxyl group. The unreacted AEAPTES was washed away by distilled water and the biochips were dried at 90°C for 30 minutes. The biochips were then activated by 10% glutaraldehyde dissolved in distilled water for 1 hour at room temperature with light avoidance and electrical field. The electrical field ensures the orientations of AEAPTES and glutaraldehyde are correct[27]. After washed away the unreacted glutaraldehyde, the unreacted hydroxyl groups of the silicon dioxide were eliminated by 10 minutes of ultraviolet light. At last, 2.5 μg/ml of anti-NGAL monoclonal antibody with 0.25% BSA in PBS was added to the well at 4°C for 12-16 hours. The biochip was blocked with 1% BSA at room temperature for 1 hour before use.

20

2.7 Quantification of NGAL of AKI patients and non-AKI control urine by Si-NW FET biochip

After functionalizing the surface of the SiNW-FET biochip and blocking, the biochip was connected to the Keithley 6485 Picoammeter. Because Si-NW FET biochip is electro-sensing based technique, after washing away 1 % BSA, the biochip was immersed in 1X PBS which the pH is adjusted to 6, lower than common IgG isoelectric point. After connecting to the picoammeter, the FET biochip was incubated in 1X pH 6 PBS for 8 minutes until the signal being stable. The measurement included four parts, 8 minutes-incubation in 1X pH6 PBS, 8 minutes-incubation in 0.01X pH6 PBS, 8 minutes-incubation of urine samples followed by 0.01X pH6 PBS wash, and 8 minutes-incubation in 0.01X pH6 PBS. At the beginning, 8 minutes' current will be recorded to evaluate the stability of the Si-NW FET biochip. If the biochip is available, the 1X pH 6 PBS will be substituted to 0.01X pH 6 PBS and measured for 8 minutes. After another 8 minutes' record, the 0.01X pH 6 PBS will be drew away and urine samples will be added to the well which are ten times diluted in the end. The urine samples will be incubated for 8 minutes. After 8 minutes-incubation, the well will be washed by 0.01X pH 6 PBS for at least five times and immersed in 0.01X pH 6 PBS. All the buffers and samples should be in contact with the AgCl electrode to avoid interruption of the circuit. The current change between two 0.01X pH 6 PBS stages indicated the levels of NGAL in samples, which can

be calculated by standard curve ranging from 1 to 400 ng/mL. Moreover, because of

drifting effect, Δ amp was calibrated with the average of slopes of four sections.

2.8   Statistical analysis

Student's t test was used to determine the significance between AKI and non-

AKI control samples. For the test, $p < 0.05$ was considered statistically significant. The

odds ratio (OR) and 95% confidence interval were estimated by Prism version 6.

Chapter 3. Results
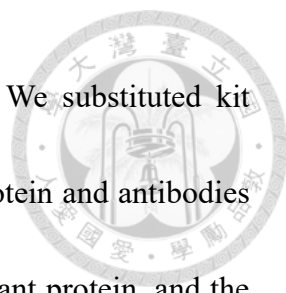
3.1 Purification of recombinant protein

In order to detect AKI faster and easier, we would like to develop SiNW-FET

biochip for NGAL quantitation. Before the development, an ELISA for NGAL

quantitation was established as a golden standard to compare with. Recombinant protein

was purified for establishing the ELISA. After transformation of the plasmid pET-28a

into E. coli strain BL21, BL21 was induced with 1 mM IPTG. An obvious band about 25

kD, the size of NGAL, was found and the target protein existed in supernatant as expected

(Figure 1a). Next, Ni^{2+}-chelating sephaorse beads, which could bind proteins in the

supernatant, was used. We used different concentration of imidazole to elute the protein.

In this study, 20 mM and 150 mM imidazole were used for washing away the unwanted

protein and 500 mM imidazole was used to elute the target protein (Figure 1b). Next, to

verify the protein, we used anti-His antibody to perform western blotting and found a

clear band after 4 hours' induction (Figure 1c). In addition, LC-MS/MS was also

performed to identify the target protein. The data showed that the unique peptide of

NGAL was found (Figure 1d).

3.2 Establishment of ELISA

After purifying recombinant protein, an ELISA system was established. In this

study, commercial kit was performed as a comparative standard. We substituted kit protein, first and secondary antibody to the purified recombinant protein and antibodies bought from R&D. Initially, kit protein was substituted to recombinant protein, and the standard curve before and after the substitution was similar (Figure 2a). Next, secondary and primary antibody was substitute from kit antibody to R&D antibody. The standard curve before and after the substitution were similar (Figure 2c). The results indicated that the establishment of the NGAL ELISA was successful. The NGAL standard curve ranged from 0 to 5000 pg/mL and the r square of the curve was 0.999 (Figure 2d). After the development of the ELISA, the urinary NGAL level of AKI patients and non-AKI controls was determined. NGAL level of AKI patients were significantly higher than of non-AKI controls (Figure 2e). All of the patient samples were provided by Dr. Wu.

3.3 Surface functionization of SiNW-FET biochip

Having finished the establishment of the ELISA, the next and the main work is to develop SiNW-FET biochip for urinary NGAL quantification. Different from traditional ELISA polystyrene plate, the antibody coating protocol of SiNW-FET relies on AEAPTES-glutaraldehyde system to carry out the process. There are four steps in SiNW-FET biochip antibody coating, hydroxylation of silicon dioxide surface, silanization, formation of glutaraldehyde linkage, and fixation of antibody.

There are four reactions in the coating process (Figure 3). At the beginning, we tested H_2O_2 and cholic acid in the first step. After testing different conditions (data not shown), 2% cholic acid was introduced (60°C, 2hr) first to produce hydroxyl group on the surface of silicon dioxide. Having finished hydroxylation of the silicon dioxide surface, 2% AEAPTES (RT, 1hr, under electrical field) was used to form the next layer. According to previous studies, APTES was the most commonly used[25, 28, 29]. However, APTES might undergo self-folding, which could disable the reaction[30]. Therefore, we chose AEAPTES for silanization. Three reactive groups of Si react with hydroxyl group and then stand on silicon dioxide. After forming the silane layer, 2.5% glutaraldehyde (RT, 1hr, under electrical field) was used to form a linkage between AEAPTES and antibody. Glutaraldehyde has two aldehyde groups, which can form covalent bonds with NH_2 groups from both AEAPTES and antibody. Finishing introducing glutaraldehyde, 2.5 μg/mL anti-NGAL antibody dissolved in 0.25 BSA (PBS-based) was used. The NH_2 group of antibody could react with one of the aldehyde group of glutaraldehyde and finished the antibody fixation process.

3.4 Establishment of measurement protocol and standard curve

The measurement of the SiNW-FET biochip includes four parts, 1X pH6 PBS, first

25

0.01X pH6 PBS, sample incubation followed by 0.01X pH6 PBS wash, and second 0.01X

pH6 PBS (Figure 4a).

The first part, 1X pH6 PBS, was the stability indicator of the SiNW-FET biochip. If

the signal is instable or the drifting effect is severe, the biochip is not available. If the

biochip is stable, 1X pH6 PBS will be change to 0.01X pH6 PBS. After incubation in

0.01X pH6 PBS (8 minutes), 0.01X pH6 PBS was changed to urine samples (8 minutes).

After incubation of urine sample, the well was washed by 0.01X pH6 PBS and immersed

in 0.01X pH6 PBS for 8 minutes. The difference between two sections of 0.01X pH6 PBS

indicated the current change (Δ amp), which was altered by the bound proteins. Therefore,

by calculate the degree of current decrease, we could know the concentration of NGAL

of the samples.

Specificity test had been performed to exclude non-specific binding. 1% BSA

was tested and the data showed that there was almost no current change after the binding

(Figure 4b). In addition, different dilution factor was tested. After testing different dilution

factor, only the urine diluted over 10 times had no matrix effect (Figure 4c). All the urine

tested in this study had the dilution factor of 10.

Before applying the SiNW-FET biochip to clinical samples, a standard cure was

established. Based on the ELISA data, NGAL concentration of most AKI patients were

higher than 100 ng/mL, and the limitation of the SiNW-FET biochip range from 1ng/mL

to 400ng/ML. Consequently, there are four concentrations in the standard curve, 1 ng/mL,

10ng/mL, 100ng/mL, and 400ng/mL (Figure 4d). By using this standard curve, we

measured urine samples from six AKI patients and six non-AKI controls.
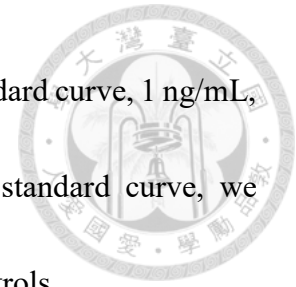
3.5　　NGAL level quantification of AKI and non-AKI

samples

A total of 7 AKI samples and 5 non-AKI samples were measured. Each samples

were repeated three times. Take chip 299 for example, NGAL level of AKI patient no. 27

was determined (Figure 5a). The current of the SiNW biochip decreased by $7.241*10^{-7}$

after 8 minutes' urine incubation, which was caused by the binding of NGAL molecules

to the antibodies. By calculating the current decrease with the standard curve, we could

know the NGAL level of the urine was 2620.5 ng/mL. In this study, 7 AKI samples and

5 non-AKI urine samples were quantified by the SiNW-FET biochip and each

measurement was repeated three times. By using the SiNW-FET biochip system, AKI and

non-AKI samples could be significantly discriminated with a p value of 0.0001 (Figure

5b). For AKI samples, NGAL levels measured by SiNW-FET biochip ranged from

approximately 1500 ng/mL to 4000 ng/mL (Table 1). On the contrary, NGAL level of four

non-AKI controls quantified by SiNW were 0 ng/mL, with an exception that non-AKI

No.3 was 442.9 ng/mL (Table 2). We compared data from both ELISA and SiNW-FET

biochip, and found that although NGAL levels from SiNW-FET biochip is higher than

from ELISA, both data showed high correlation (Table 1 and Table 2).
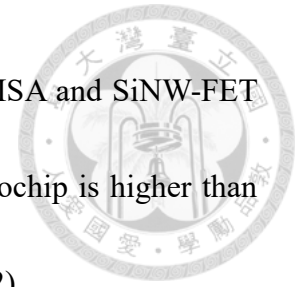
3.6   Conclusion
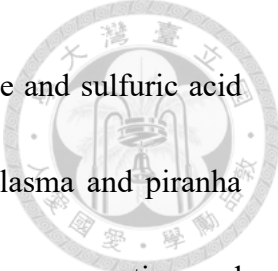
In this study, we developed a SiNW-FET biochip, which could quantify NGAL

level of AKI and non-AKI samples. Compared to traditional coating process, we modified

the first two reactions, hydroxylation and silanization. In hydroxylation, cholic acid had

been used to generate hydroxyl groups without dealing too much damage to the silicon

dioxide. Next, AEAPTES, which is still able to perform reaction after self-catalysis, had

been used in silanization. In addition to cholic acid and AEAPTES, electrical field was

applied to AEAPTES and glutaraldehyde to correct the molecular orientation. These

modifications make the SiNW-FET biochip more stable than before. We used the

modified SiNW-FET biochip to quantified urine NGAL level of 7 AKI and 6 non-AKI

samples, and the data showed similar results to ELISA data, indicating the biochip is

available for clinical usage.

Chapter 4.   Discussion
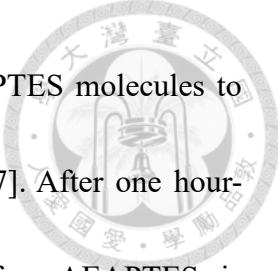
SiNW-FET has the benefits of fast and real-time detection, ultra-sensitivity and specificity, label-free, and label-free. In addition, SiNW-FET can be used in a variety of aspects, protein-protein interaction, DNA hybridization, and peptide-small molecule interaction. According to previous studies, this technique was used in different biomarkers, such as troponin for myocardio infarction, prostate specific antigen for prostate cancer, and cytokeratin 19 fragment for lung cancer[31, 32]. However, because of its instability and uneven distribution of antibody, most of these researches did not apply the SiNW-FET sensor to clinical samples[29]. In this study, we modified the traditional AEPES-glutaraldehyde system and therefore improve its performance. We not only set up standard curve but also quantified NGAL level of clinical urine samples.

The modifications of the coating protocol, including the use of cholic acid and AEAPTES, make the SiNW-FET biochip have better performance. In the first step, cholic acid was used to generate hydroxyl group. According to previous study, there are several methods to produce hydroxyl group, including hydrogen peroxide, sodium hydroxide, cholic acid, oxygen plasma, piranha solution, and sulfuric acid[33]. Oxygen plasma is improper for our chip because the silicon wafer was already cut into pieces and embedded onto the PCB, and oxygen plasma is so strong that can penetrate the plastic part of the

PCB. In addition, piranha solution is a mixture of hydrogen peroxide and sulfuric acid that could erode the wire of the FET biochip. Therefore, oxygen plasma and piranha solution are inadequate. Initially, H_2O_2 was used for hydroxyl group generation and APTES was used in silanization process. The Δ amp of this treatment was at the level of 10^{-10} (data not shown). In order to increase the signal, the thickness of SiO_2 was reduced to 24 nm and the level of Δ amp could achieve 10^{-7} to 10^{-6}. We tested the H_2O_2, NaOH and cholic acid to generate hydroxyl group and found that cholic acid could generated hydroxyl group without dealing damage to the biochip. In the H_2O_2 group, the r square of standard curve range from 0.8 to 0.94, however, in the cholic acid and NaOH group, the r square reached 0.99 (data not shown). Although both NaOH and cholic acid groups had few drifting effect ($<8\times10^{-10}$ amp/sec, data not shown), NaOH could possibly corrupt SiO_2, therefore we chose cholic acid in the hydroxylation process.
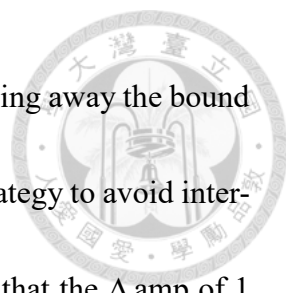
Having finished hydroxylation of the silicon dioxide surface, the next step is silanization. In previous studies, (3-aminopropyl) triethoxysilane (APTES) was used in SiNW-FET coating processes[28, 34, 35]. The three functional group around the silicon of APTES can react with hydroxyl group of the surface, while the amine group on the other side can react with glutaraldehyde which will be introduced later. However, the amine group of APTES can fold back and interact with the central silicon[30, 36]. Thus, AEAPTES, which is modified from APTES, was chosen and used in the silanization

30

process. Moreover, an electrical field was used to extend the AEAPTES molecules to prevent self-folding or interactions between adjacent AEAPTESs[27]. After one hour-incubation, the well was washed by distilled water because free AEAPTES is hydrolytically instable.

After silanization, glutaraldehyde was introduced to form linkage between AEAPTES and antibody. During the incubation of AEAPTES and glutaraldehyde, electrical field was applied to make sure the orientation of the molecules is correct. After finishing incubation of glutaraldehyde, ultraviolet radiation was used to eliminate the unreacted hydroxyl groups. According to previous study, drifting effect is probably the consequence of reaction between buffer ions and unreacted hydroxyl groups on the silicon dioxide[37]. Therefore, by eliminating the unreacted hydroxyl groups, drifting effect might become minor. After the UV radiation, antibody was introduced. Unlike traditional coating protocol, we used 0.25% PBS-based BSA as solvent. The addition of BSA prevents two antibodies getting too close. All of these modifications help the SiNW-FET chips more stable and ameliorate the drifting effect so that the chip could be used in quantifying clinical samples.

However, there are still some problems. For example, the thickness of the silicon dioxide is not consistent in all biochip. Because of the variation of the silicon dioxide thickness, the baseline current differs from chip to chip. Therefore, we tried to use single

biochip to set up standard curve and quantify NGAL level after stripping away the bound

proteins. Quantification NGAL level by a single biochip is a good strategy to avoid inter-

chip variation, but two major issues cannot be solved. The first was that the Δ amp of 1

ng/mL was much larger than Δ amps of 10, 100, and 400 ng/mL. Even though same

concentration of recombinant protein was added in serial, the first Δ amp was larger than

the others. Despite of that challenge, the recipe of stripping buffer was difficult to be

determined. We used glycine-HCl (pH 3.5) and adjust its pH to the most suitable one.

However, low pH stripping buffer could deal damage to the biochip wire while high pH

buffer did not have efficient stripping ability. Due to these two reason, we used different

biochips to set up standard curve and quantify urine NGAL level.

In addition to inter-chip variation, the drifting effect may also affect the results

of the measurement. In general, drifting effect is the consequence of very small cracks on

the SiO_2. When Electrons or ions penetrate these small cracks of the SiO_2 layer, the

resistance of the Si substrate changes slowly. To improve that, different materials might

be tested as dieletric layer in the future to prevent the penetration. Despite we have

decreased the level of drifting, it did not disappear completely. In the future, the

mentioned issues need to be solved. First, how to calibrate the variation of the silicon

dioxide thickness. Second, how to calibrate or improve the error caused by drifting. Third,

since the chip is small and designed for portable, any vibration or shake might affect the

stability. Consequently, we should increase the stability and the yield rate of the chip.

Chapter 5.   Tables and Figures
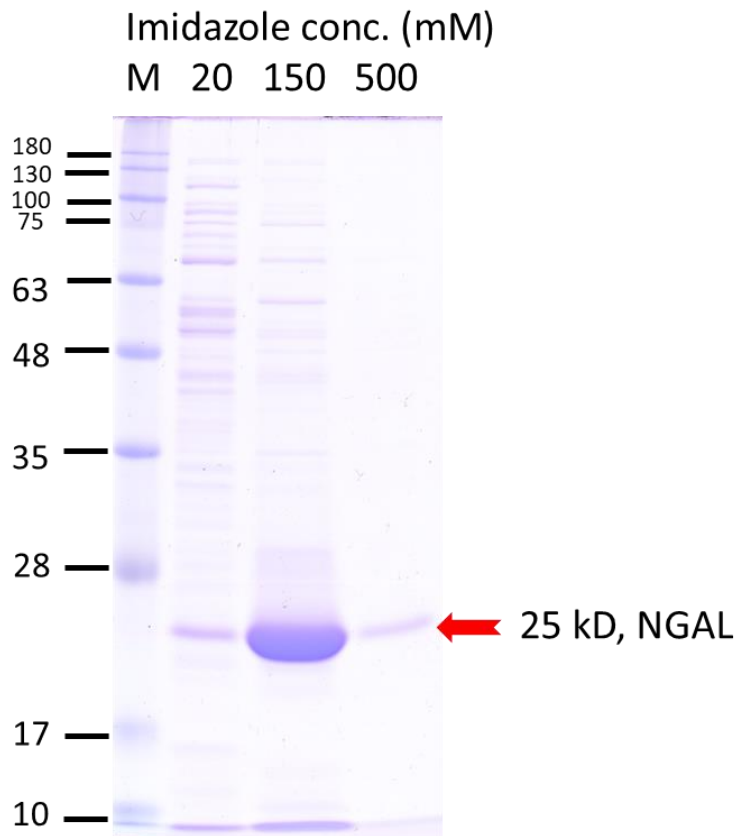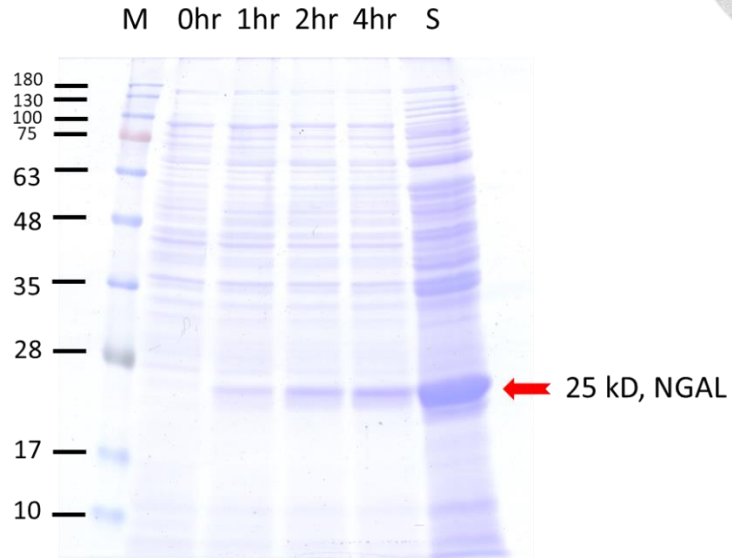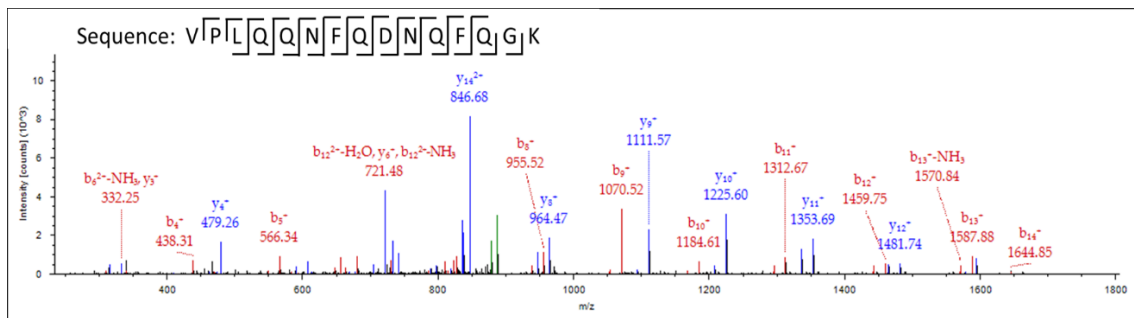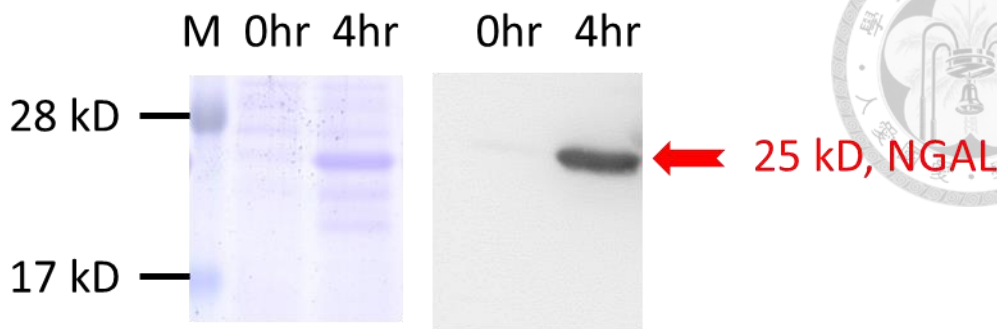
Figure 1. Purification of NGAL recombinant protein.

(A) E. coli BL21 transformed with pET-289(a) containing *lcn2* was induced with 1mM IPTG. E. coli with different induction time was collected and analyzed by SDS-PAGE. The red arrow showed that NGAL protein was induced by IPTG and the majority of NGAL protein existed in the supernatant. M, marker. S, supernatant. **(B)** After induction, E. coli were lysed and centrifugated to obtain the supernatant. Proteins in the supernatant bound to Nicole beads and was eluted by different concentrations of imidazole. The red arrow indicated that most of the NGAL recombinant protein was eluted by 150 mM imidazole. **(C)** Western blotting was performed to confirm the purified protein. Anti-his antibody was used in the assay. **(D)** LC-MS/MS was performed to verify the purified protein. The unique peptide of NGAL was identified by LC-MS/MS

Correlation coefficients: 0.999

Correlation coefficients: 0.995

36
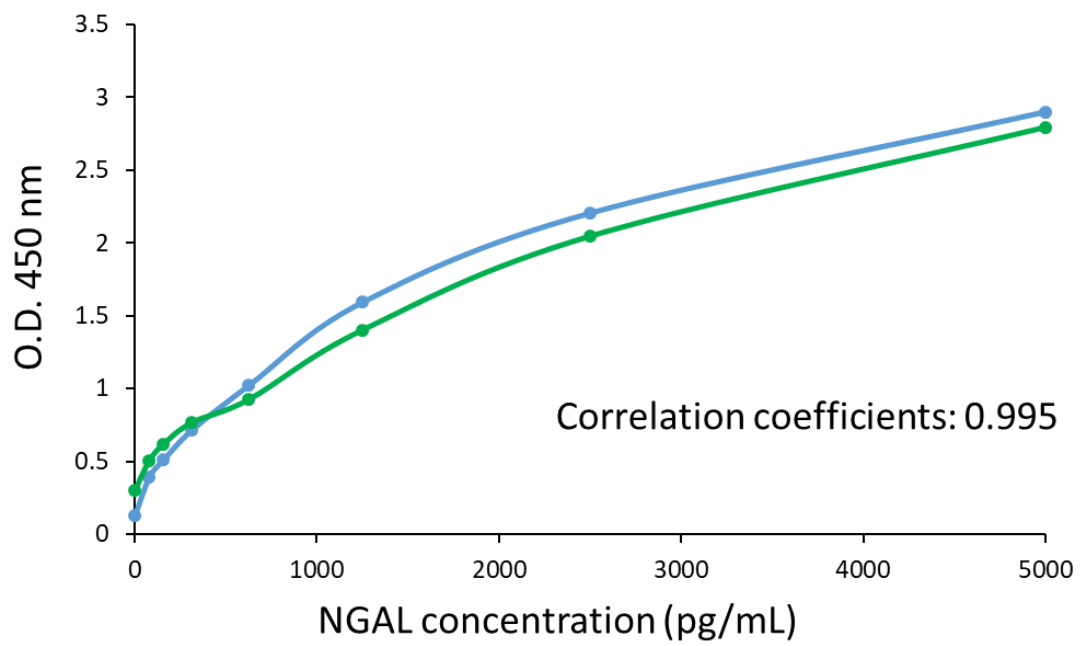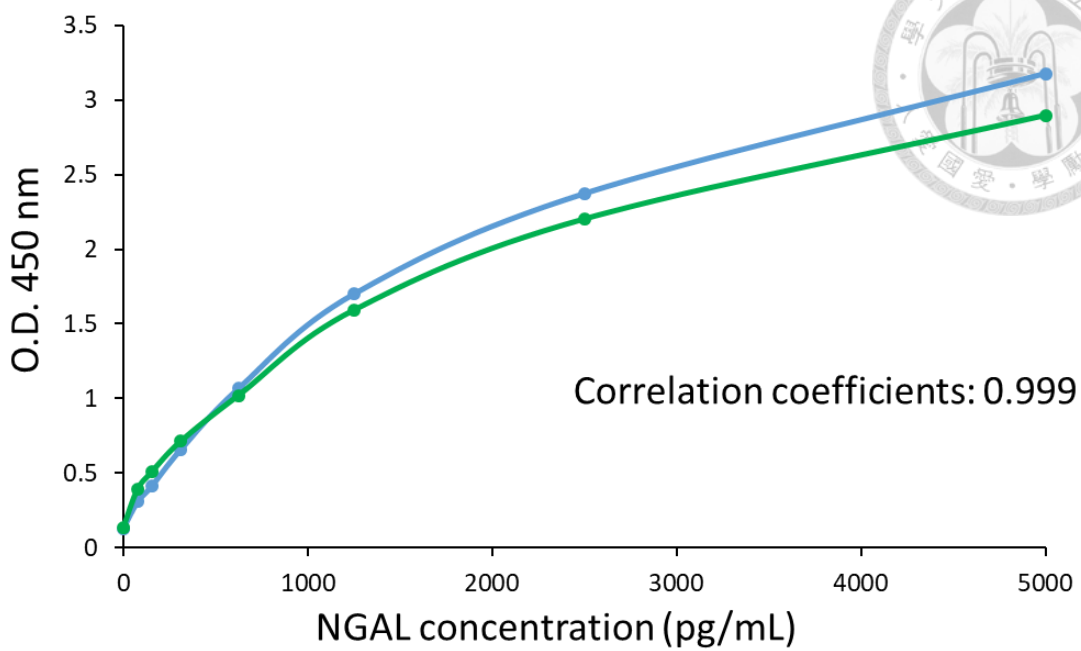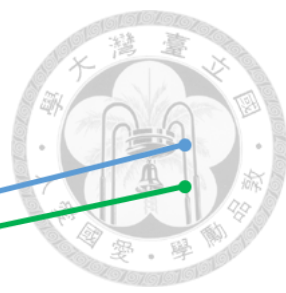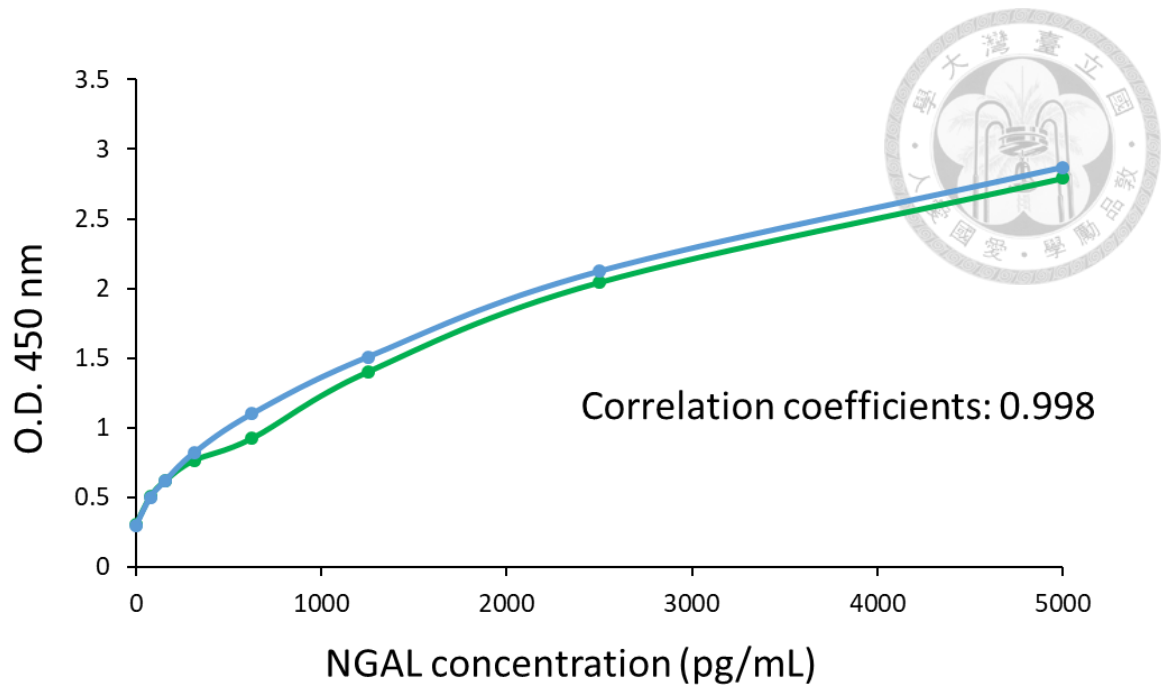
Figure 2a-c. Establishment of NGAL ELISA and quantification of NGAL level.
(A) to (C) To establish an ELISA, a commercial kit ELISA was performed first and the reagents were substituted one by one. The orange curves represented before substitution while the green curve represents after substitution. (A) Kit protein was substituted to purified protein. (B) Kit secondary antibody was substituted to R&D secondary antibody (C) Kit first antibody was substituted to R&D first antibody.
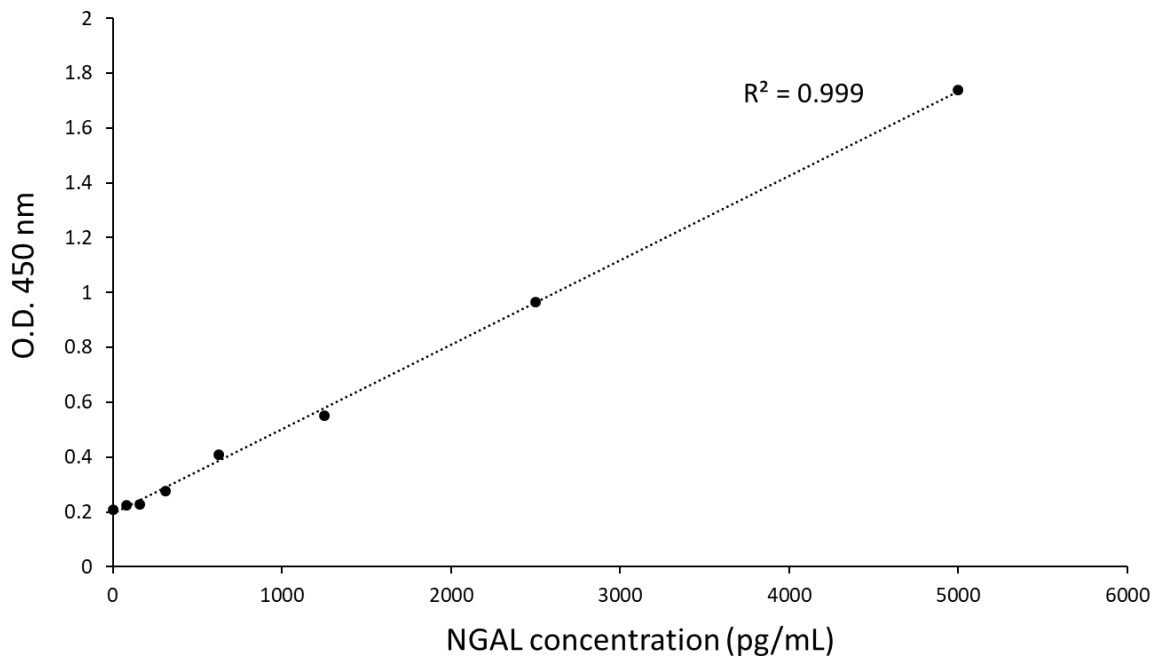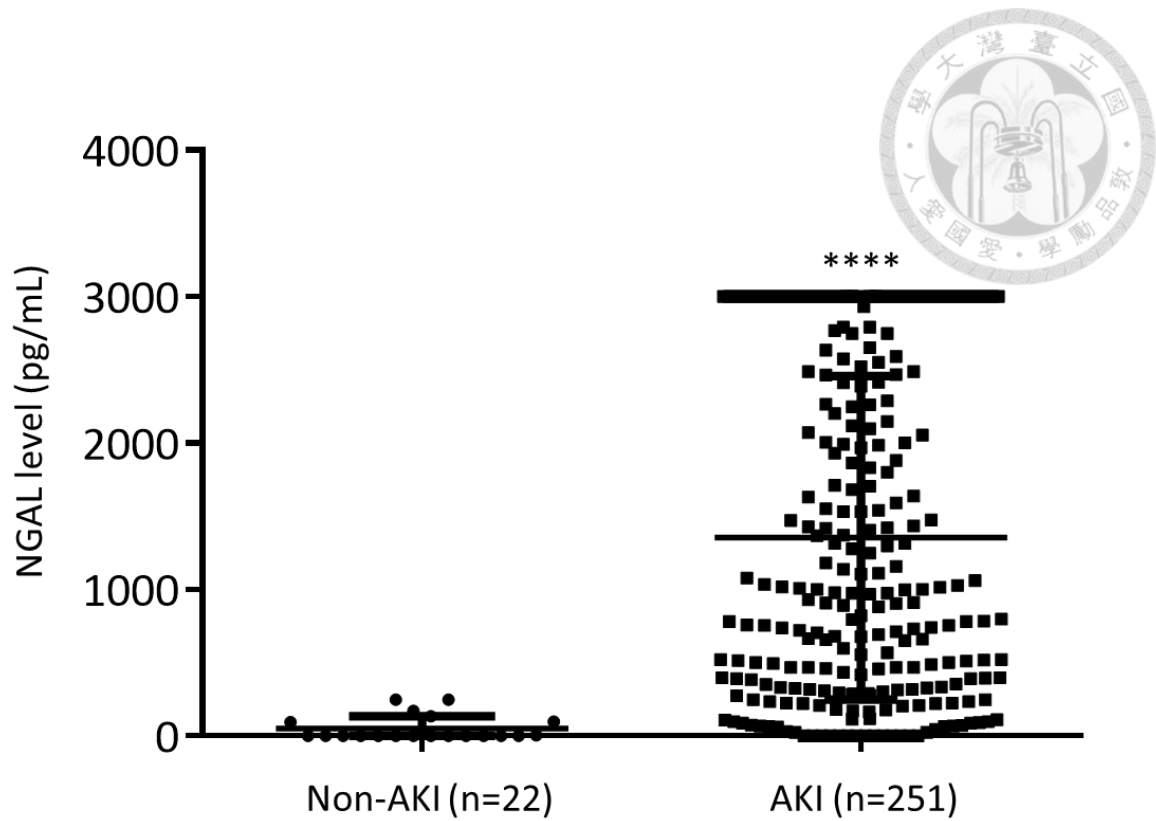
Figure 2d-e Establishment of NGAL ELISA and quantification of NGAL level.
(D) Standard curve of the established NGAL ELISA. **(E)** A total of 251 AKI and 22 non-AKI urine samples were analyzed by ELISA. ****$p<0.0001$.
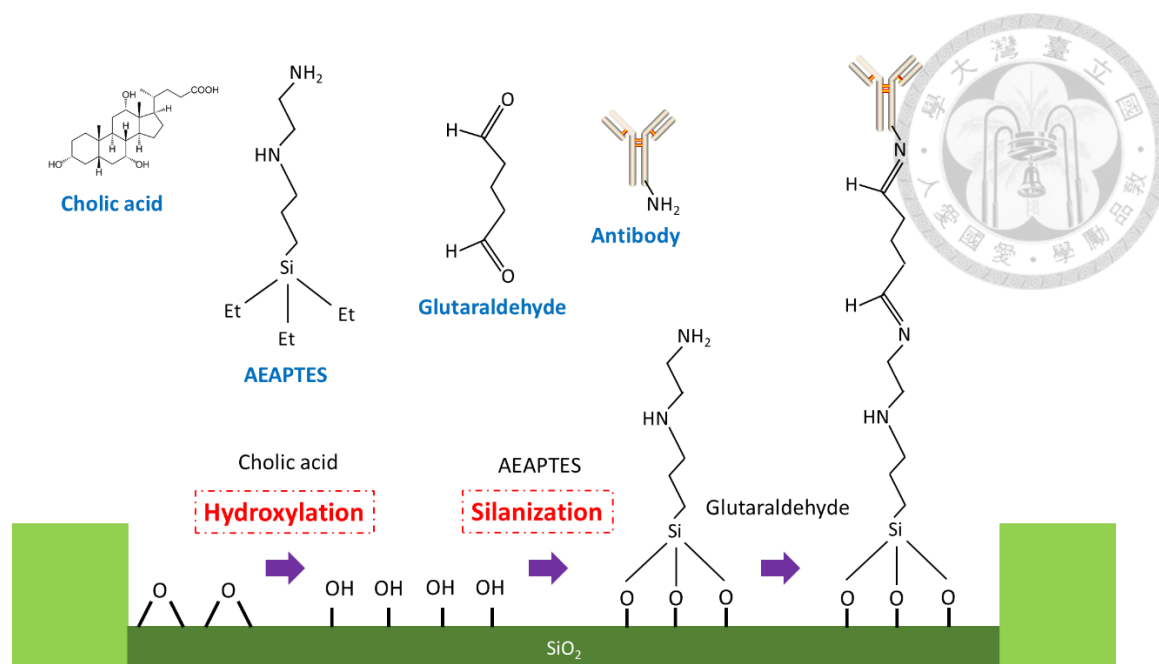
Figure 3 Diagram of coating protocol of SiNW-FET biochip.

The coating protocol included four parts, production of hydroxyl groups, silanization, addition of glutaraldehyde, and fixation of antibodies.
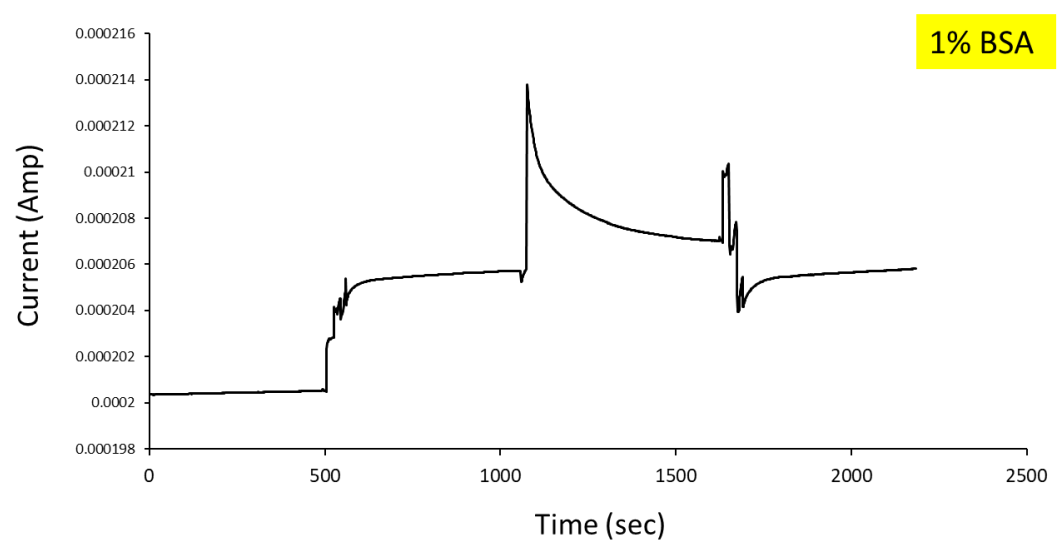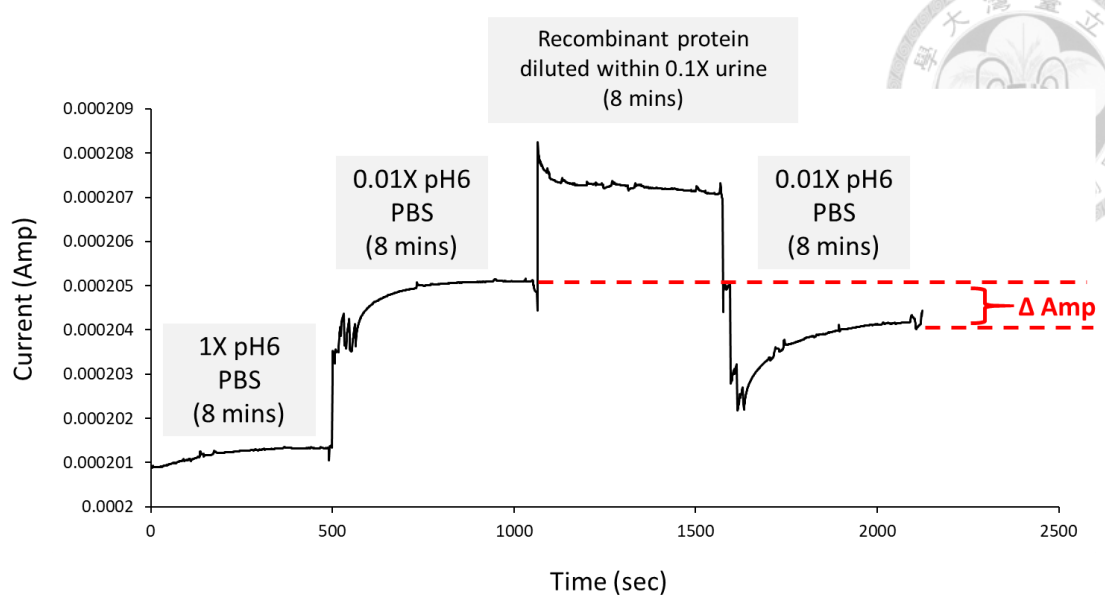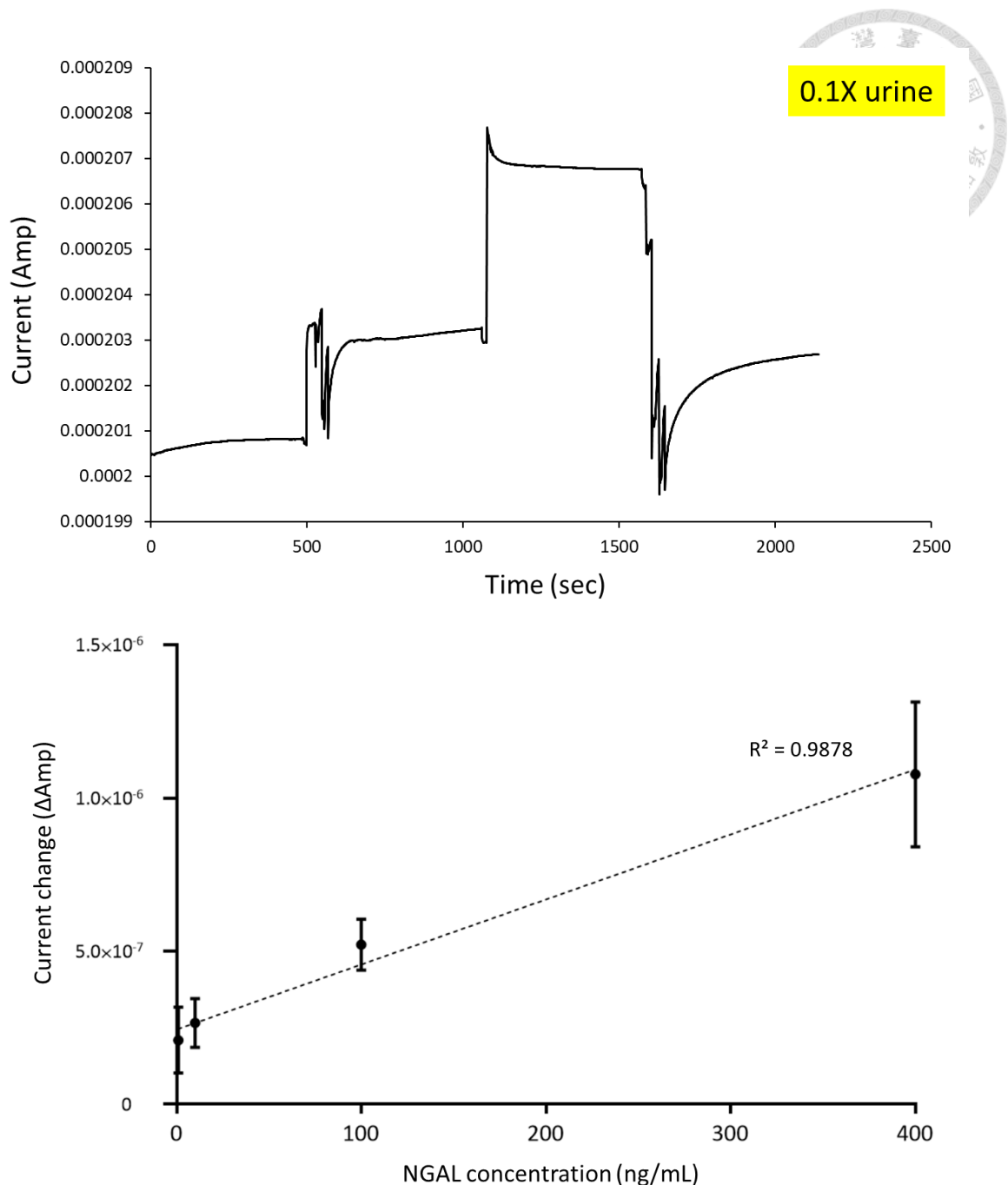
Figure 4. Determination of the operating protocol and dilution factor.

(A) As the figure showed, the measurement was divided into four parts. The protein level was determined by the difference between two sections of 0.01X pH6 PBS. **(B)** 1% BSA was added in the third section of the measurement. There was no apparent difference between two 0.01X pH6 PBS sections, which means non-specific binding did not occur. **(C)** 0.1X urine was added in the third section of the measurement. After trying different dilution ratios, only the urine samples diluted more than 10 times showed similar pattern to BSA control. (D) Based on the operating protocol, a standard curve, ranged from 1 ng/mL, 10 ng/mL, 100ng/mL, to 400 ng/mL, was set up.

41

doi:10.6342/NTU201803988
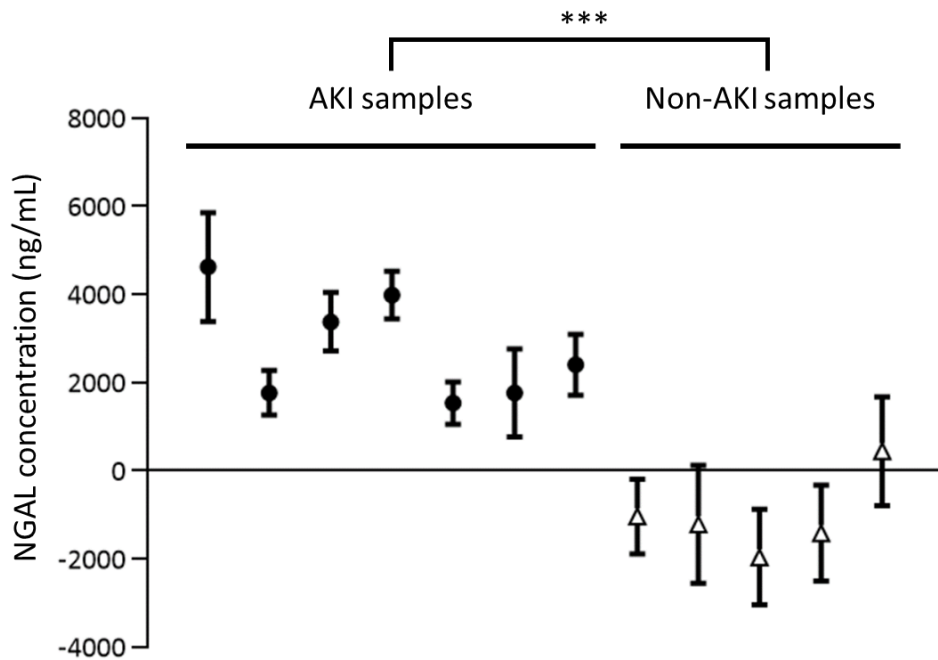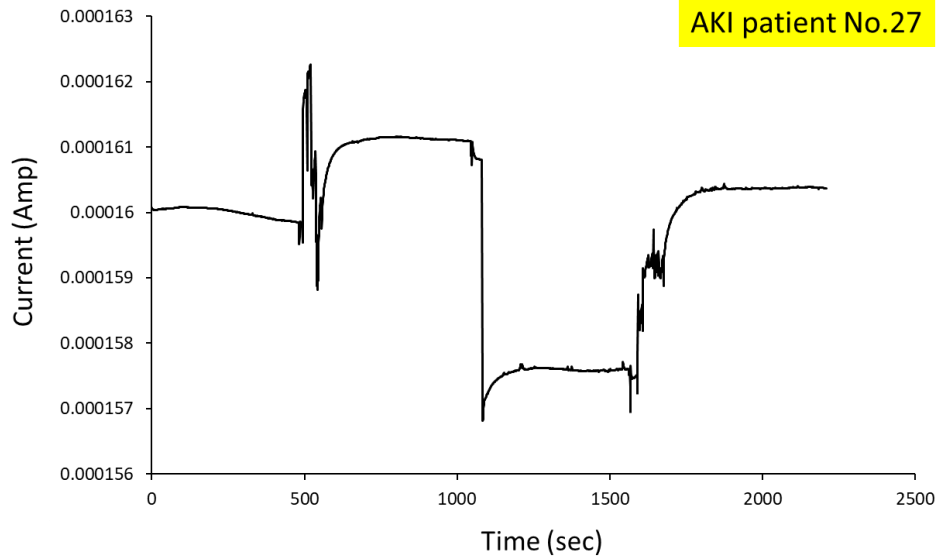
Figure 5. Quantification of NGAL level by SiNW-FET biochip.

(A) AKI patient no. 27 was analyzed by SiNW-FET biochip 299. According to the curve, the difference between two 0.01X pH6 PBS section was $7.241*10^{-7}$. By calculating with the standard curve, the NGAL level of AKI patient no. 27 urine was 262.05 ng/mL. **(B)** 7 AKI (solid dots) and 5 non-AKI samples (triangles) were analyzed by the SiNW-FET biochip. ***$p<0.001$

Table 1. Comparison of NGAL level of AKI patients between SiNW-FET chip and ELISA

AKI patient no.	NGAL level from SiNW-FET chip (ng/mL)	NGAL level from ELISA (ng/mL)	CV(%) of the SiNW-FET data
31	>4000	>3000	17.9
33	1766.6	1277.6	14.9
27	3377.45	2575	12.5
34	3984.7	2464.8	8.8
45	1534.25	1592.7	15.5
44	1768.7	1863.9	29.5
168	2408.1	1296.75	16.5

Table 2. Comparison of NGAL level of non-AKI controls between SiNW-FET chip and ELISA
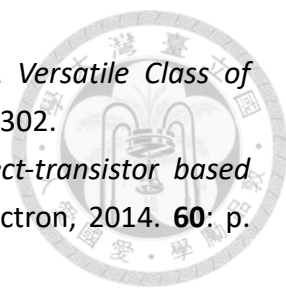
Non-AKI control no.	NGAL level from SiNW-FET chip (ng/mL)	NGAL level from ELISA (ng/mL)
1	0	0
2	0	0
7	0	0
8	0	0
3	442.9	249

References

1. Devarajan, P., *Review: neutrophil gelatinase-associated lipocalin: a troponin-like biomarker for human acute kidney injury.* Nephrology (Carlton), 2010. **15**(4): p. 419-28.

2. *Acute renal failure.pdf.*

3. fundamentalsofnursingblog. *Three subtypes of AKI.* December 15, 2016; Available from: https://fundamentalsofnursingblog.wordpress.com/2016/12/15/acute-kidney-injury/.

4. Osmosis, *Prerenal AKI.* 2016.

5. Osmosis, **Intrarenal AKI.** 2016.

6. Osmosis, *Postrenal AKI.* 2016.

7. *Postrenal AKI (Causes).* Available from: https://en.wikipedia.org/wiki/Acute_kidney_injury.

8. Lopes, J.A. and S. Jorge, *The RIFLE and AKIN classifications for acute kidney injury: a critical and comprehensive review.* Clin Kidney J, 2013. **6**(1): p. 8-14.

9. Park, W.Y., et al., *The risk factors and outcome of acute kidney injury in the intensive care units.* Korean J Intern Med, 2010. **25**(2): p. 181-7.

10. Susan M. Dirkes, B., MSA, CCRN. *Acute kidney injury: Causes, phases, and early detection.* 2015; Available from: https://www.americannursetoday.com/acute-kidney-injury/.

11. Parikh, C.R., et al., *Urinary IL-18 is an early predictive biomarker of acute kidney injury after cardiac surgery.* Kidney Int, 2006. **70**(1): p. 199-203.

12. Xu, Y., et al., *L-FABP: A novel biomarker of kidney disease.* Clin Chim Acta, 2015. **445**: p. 85-90.

13. Vanmassenhove, J., et al., *Urinary and serum biomarkers for the diagnosis of acute kidney injury: an in-depth review of the literature.* Nephrol Dial Transplant, 2013. **28**(2): p. 254-73.

14. Mishra, J., et al., *Amelioration of ischemic acute renal injury by neutrophil gelatinase-associated lipocalin.* J Am Soc Nephrol, 2004. **15**(12): p. 3073-82.

15. Clerico, A., et al., *Neutrophil gelatinase-associated lipocalin (NGAL) as biomarker of acute kidney injury: a review of the laboratory characteristics and clinical evidences.* Clin Chem Lab Med, 2012. **50**(9): p. 1505-17.

16. Schmidt-Ott, K.M., et al., *Dual action of neutrophil gelatinase-associated lipocalin.* J Am Soc Nephrol, 2007. **18**(2): p. 407-13.

17.   *The Neutrophil Lipocalin NGAL Is a Bacteriostatic Agent that Interferes with Siderophore-Mediated Iron Acquisition.pdf.*

18.   Chakraborty, S., et al., *The multifaceted roles of neutrophil gelatinase associated lipocalin (NGAL) in inflammation and cancer.* Biochim Biophys Acta, 2012. **1826**(1): p. 129-69.

19.   Supavekin, S., et al., *Differential gene expression following early renal ischemia/reperfusion.* Kidney Int, 2003. **63**(5): p. 1714-24.

20.   Yuen, P.S., et al., *Ischemic and nephrotoxic acute renal failure are distinguished by their broad transcriptomic responses.* Physiol Genomics, 2006. **25**(3): p. 375-86.

21.   *1289.full.pdf.*

22.   *Low-cost and Ultra-sensitive Poly-Si Nanowire Biosensor for Hepatitis B Virus (HBV) DNA Detection.pdf.*

23.   Zheng, G., et al., *Multiplexed electrical detection of cancer markers with nanowire sensor arrays.* Nat Biotechnol, 2005. **23**(10): p. 1294-301.

24.   *A fully integrated hepatitis B virus DNA detection SoC based on monolithic polysilicon nanowire CMOS process.pdf.*

25.   *A-CMOS-Based-Polysilicon-Nanowire-Biosensor-for-Monitoring-the-Cardiovascular-Disease-Markers-in-Human-Serum.pdf.*

26.   Pei-Wen, Y., et al., *A device design of an integrated CMOS poly-silicon biosensor-on-chip to enhance performance of biomolecular analytes in serum samples.* Biosens Bioelectron, 2014. **61**: p. 112-8.

27.   Chu, C.J., et al., *Improving nanowire sensing capability by electrical field alignment of surface probing molecules.* Nano Lett, 2013. **13**(6): p. 2564-9.

28.   Huang, C.W., et al., *A CMOS wireless biomolecular sensing system-on-chip based on polysilicon nanowire technology.* Lab Chip, 2013. **13**(22): p. 4451-9.

29.   Chen, K.-I., B.-R. Li, and Y.-T. Chen, *Silicon nanowire field-effect transistor-based biosensors for biomedical diagnosis and cellular recording investigation.* Nano Today, 2011. **6**(2): p. 131-154.

30.   Zhu, M., M.Z. Lerum, and W. Chen, *How to prepare reproducible, homogeneous, and hydrolytically stable aminosilane-derived layers on silica.* Langmuir, 2012. **28**(1): p. 416-23.

31.   Lu, N., et al., *Ultrasensitive Detection of Dual Cancer Biomarkers with Integrated CMOS-Compatible Nanowire Arrays.* Anal Chem, 2015. **87**(22): p. 11203-8.

32.   Lei, Y.M., et al., *Detection of heart failure-related biomarker in whole blood with graphene field effect transistor biosensor.* Biosens Bioelectron, 2017. **91**: p. 1-7.

33.   Han, Y., et al., *Surface activation of thin silicon oxides by wet cleaning and silanization.* Thin Solid Films, 2006. **510**(1-2): p. 175-180.

34.   Mu, L., et al., *Silicon Nanowire Field-Effect Transistors—A Versatile Class of Potentiometric Nanobiosensors.* IEEE Access, 2015. **3**: p. 287-302.

35.   Shen, M.Y., B.R. Li, and Y.K. Li, *Silicon nanowire field-effect-transistor based biosensors: from sensitive to ultra-sensitive.* Biosens Bioelectron, 2014. **60**: p. 101-11.

36.   Nicholas, M.P., L. Rao, and A. Gennerich, *Covalent immobilization of microtubules on glass surfaces for molecular motor force measurements and other single-molecule assays.* Methods Mol Biol, 2014. **1136**: p. 137-69.

37.   Son, H.W., et al., *A strategy to minimize the sensing voltage drift error in a transistor biosensor with a nanoscale sensing gate.* Int J Nanomedicine, 2017. **12**: p. 2951-2956.

Attachments

Chips for standard curve
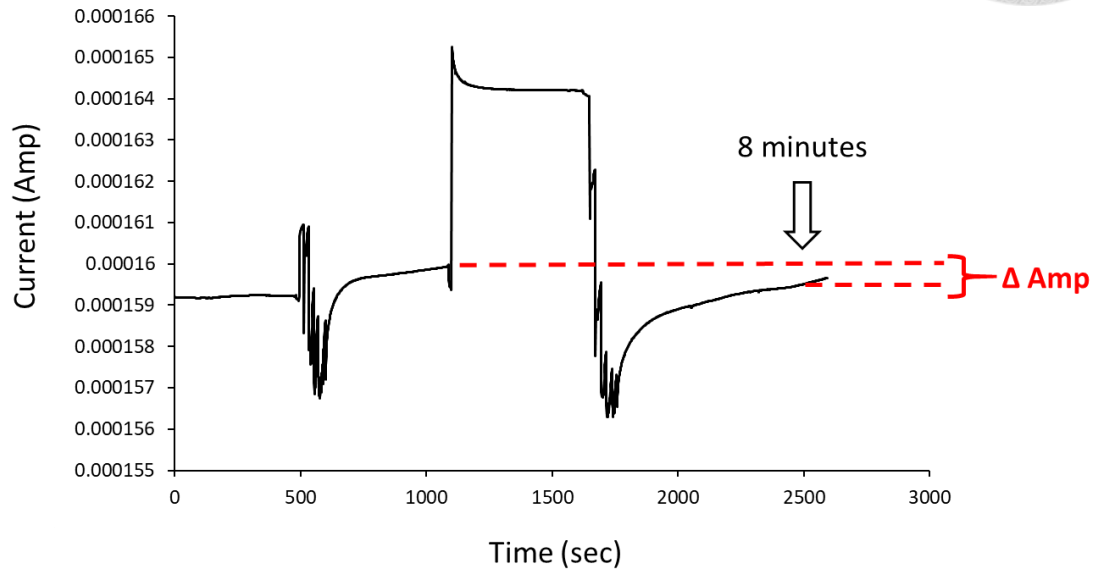
Chip 138, 1ng/mL

Chip 140, 1ng/mL

47
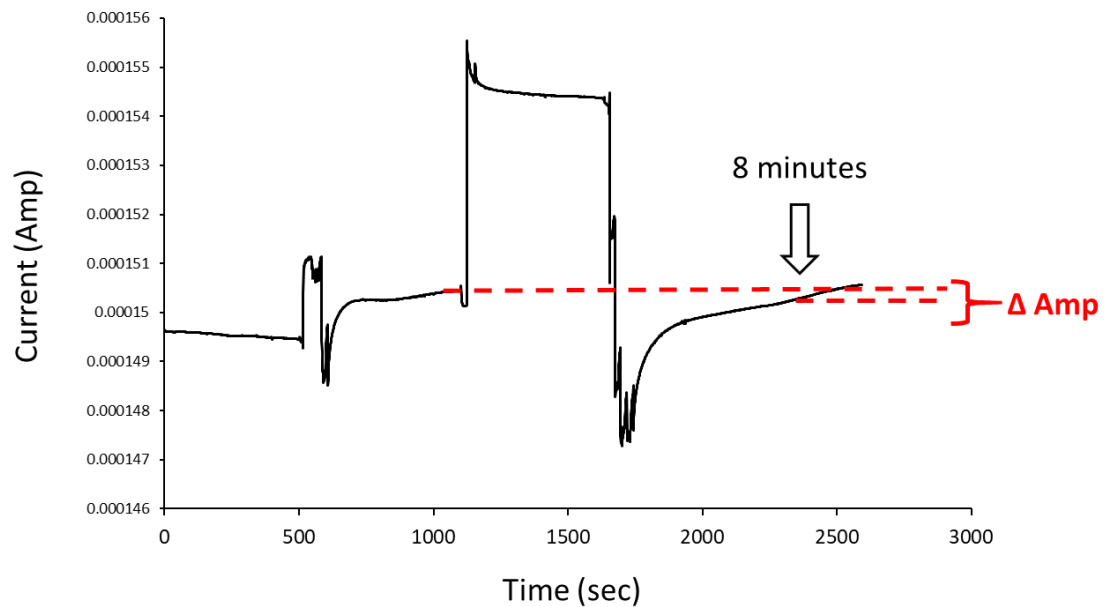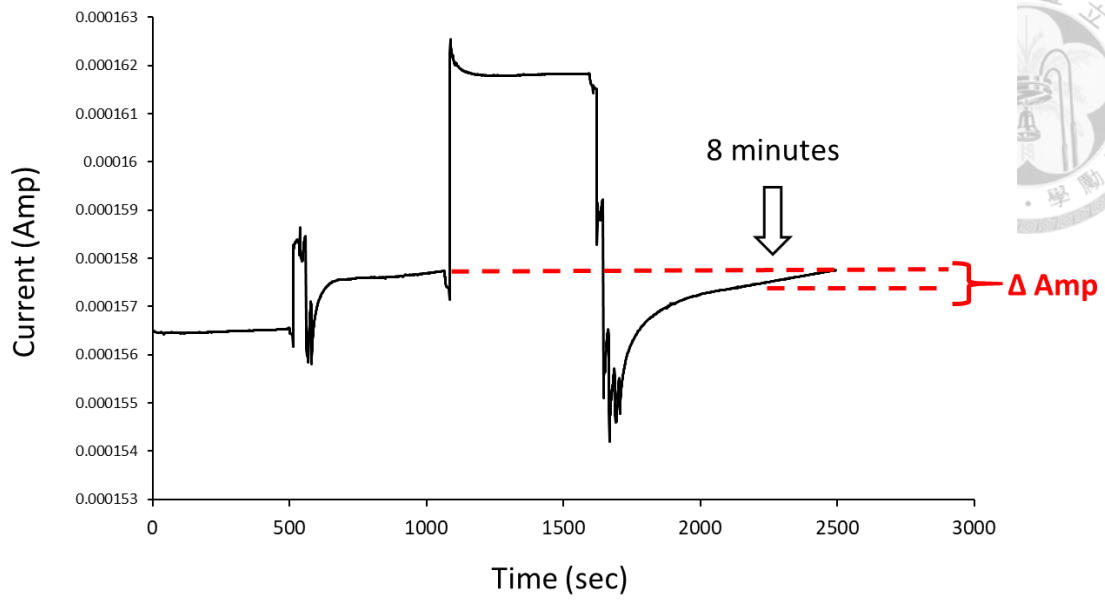
Chip 141, 1ng/mL
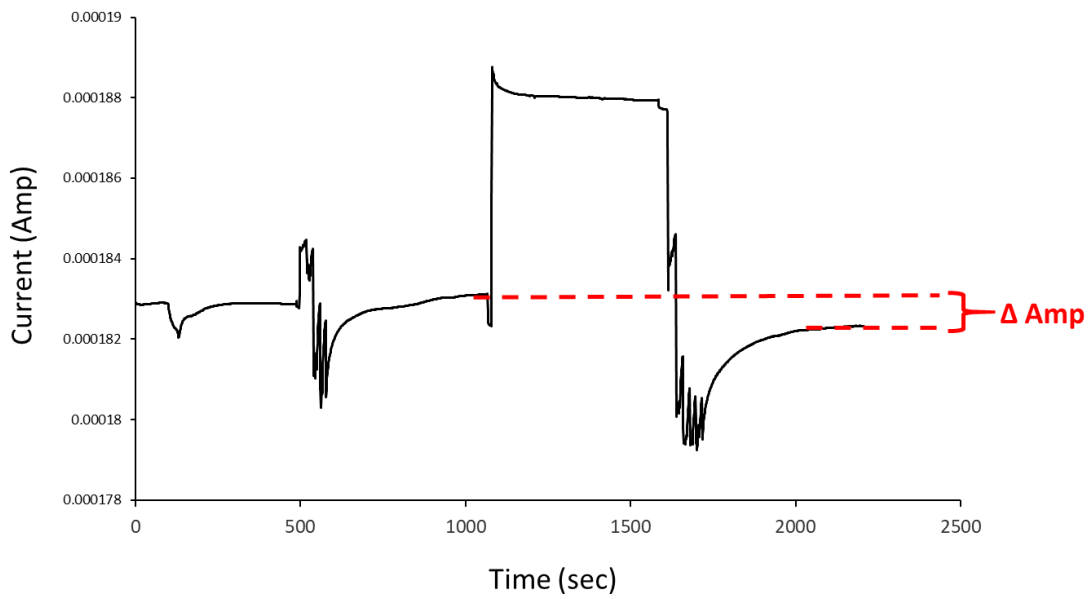
Chip 148, 1ng/mL
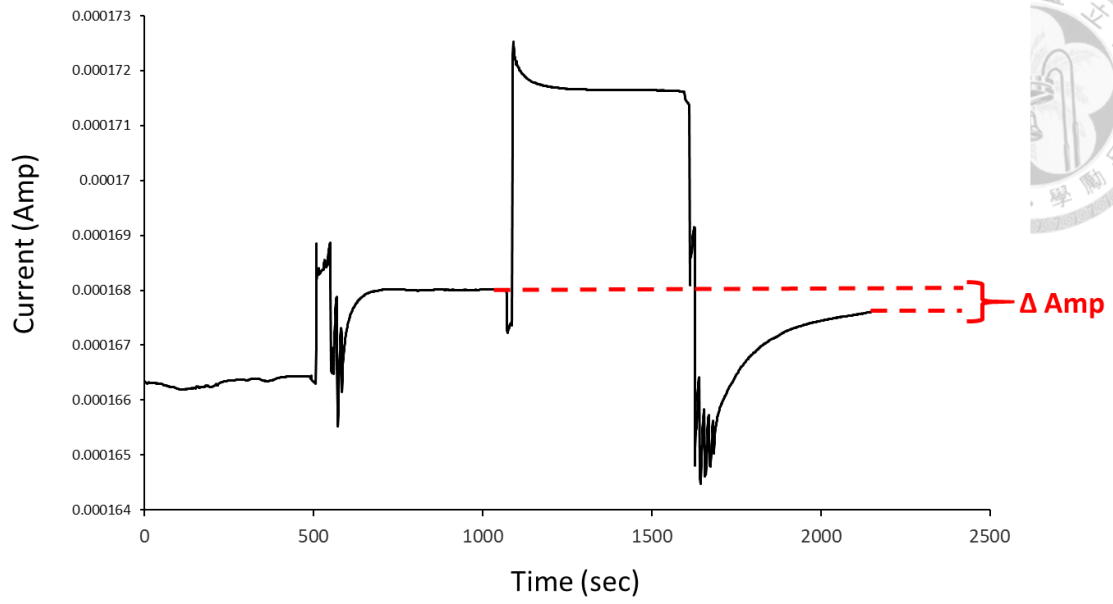
Chip 151, 10ng/mL

Chip 160, 10ng/mL

49
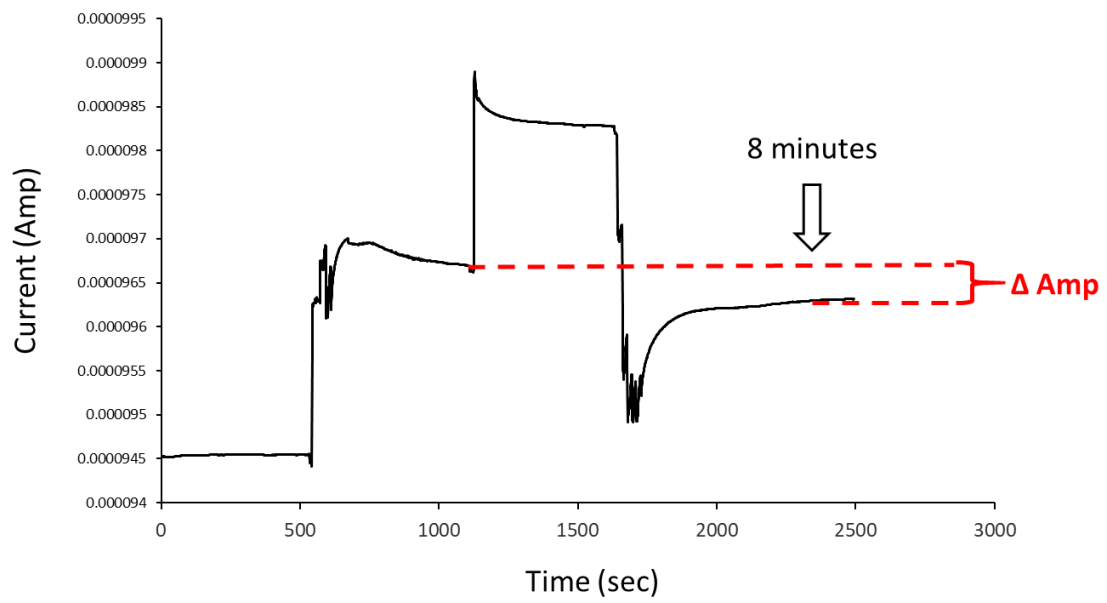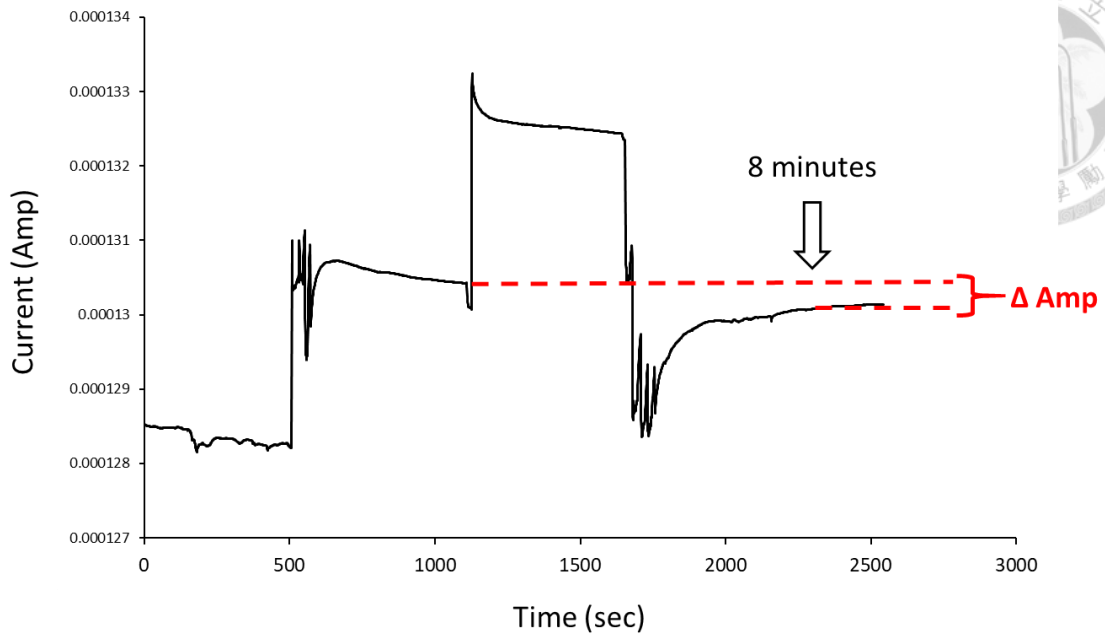
Chip 163, 10ng/mL
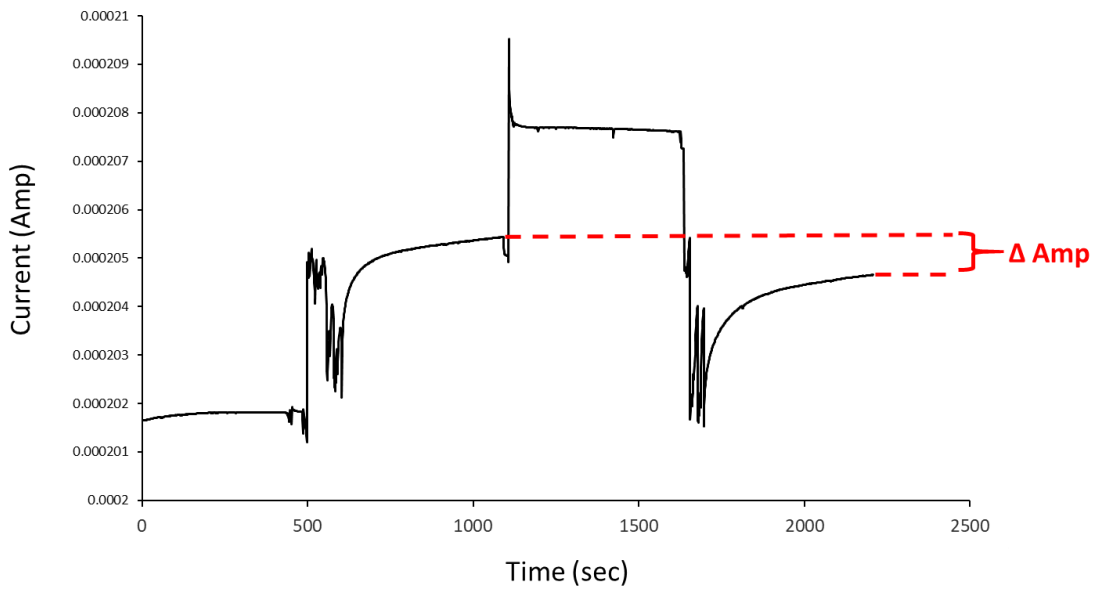
Chip 105, 100ng/mL
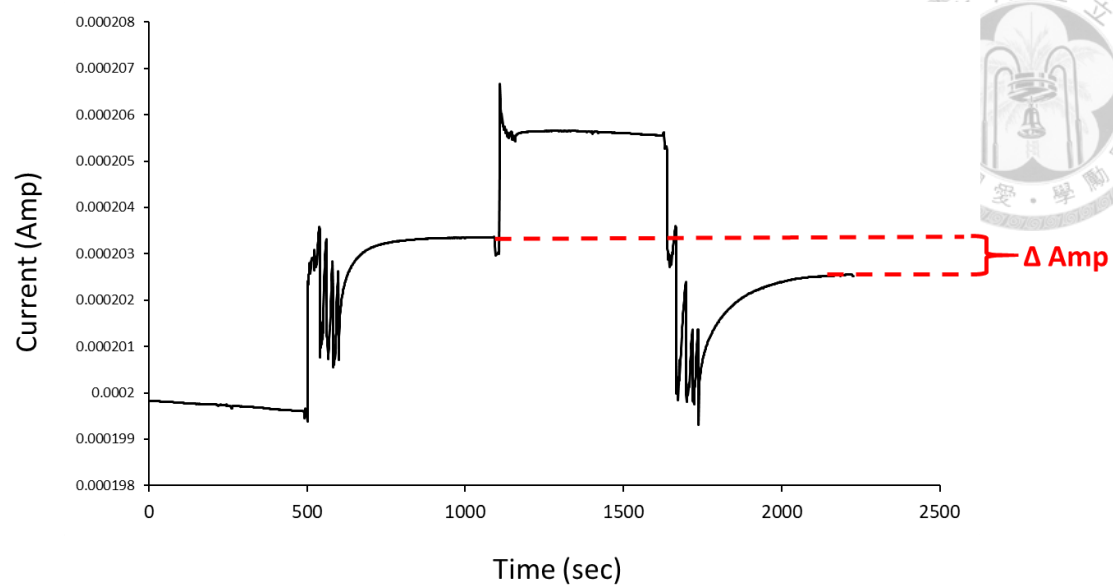
Chip 107, 100ng/mL

Chip 167, 100ng/mL

51
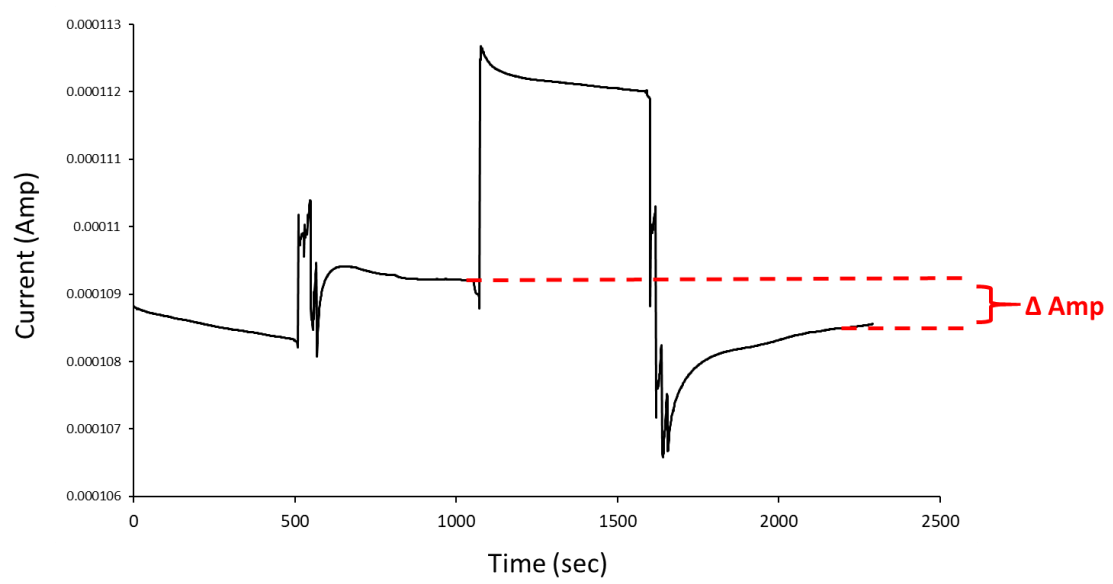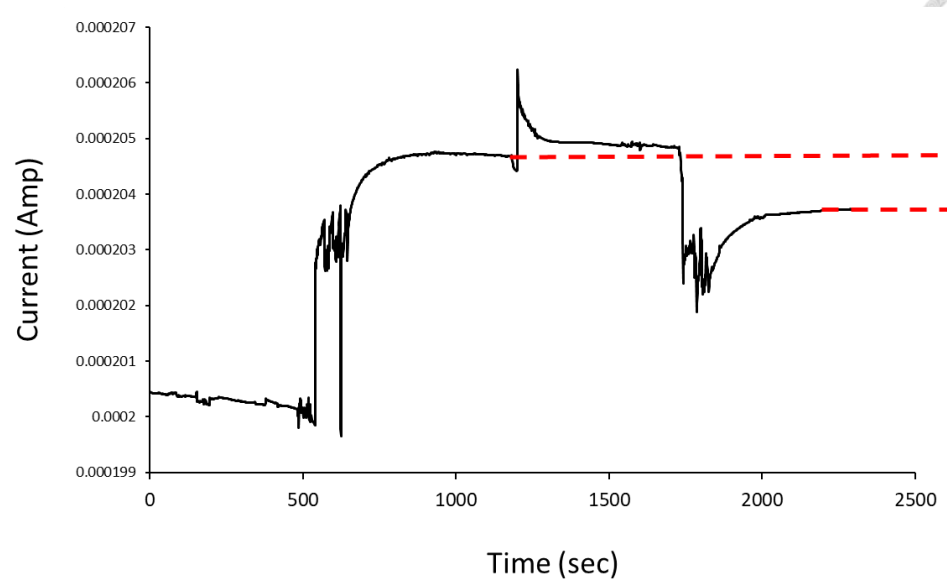
Chip 87, 400ng/mL

Chip 88, 400ng/mL

52
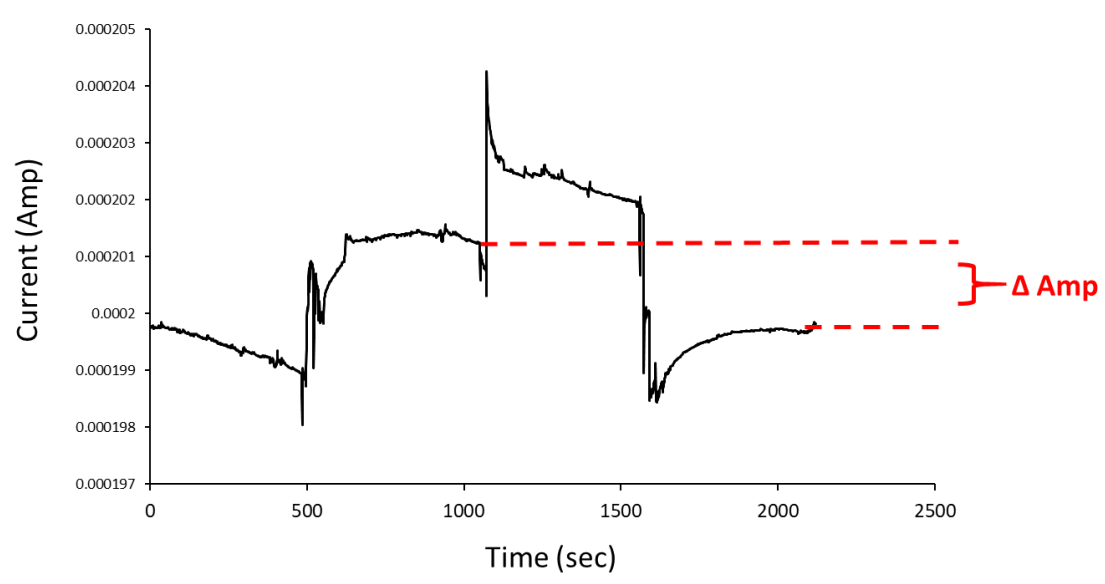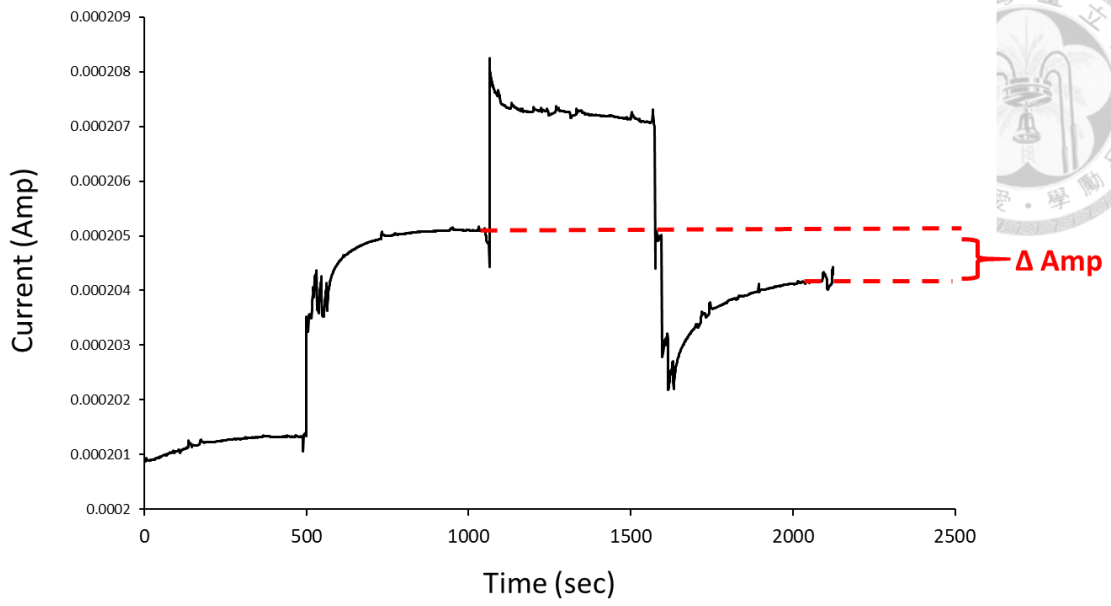
Chip 90, 400ng/mL

AKI samples
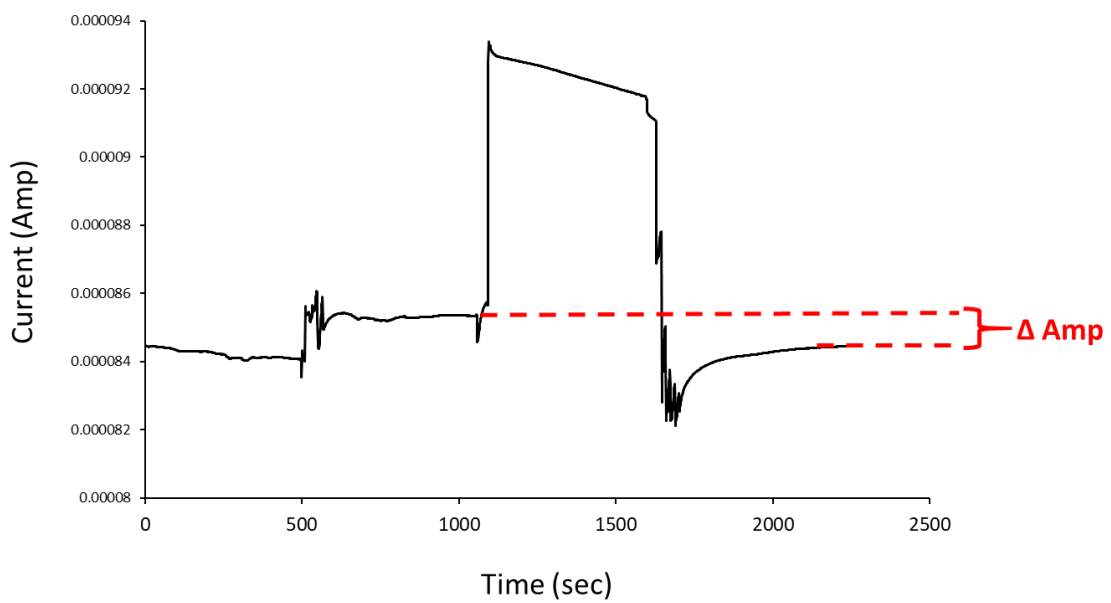
Chip 192, AKI patient No. 31
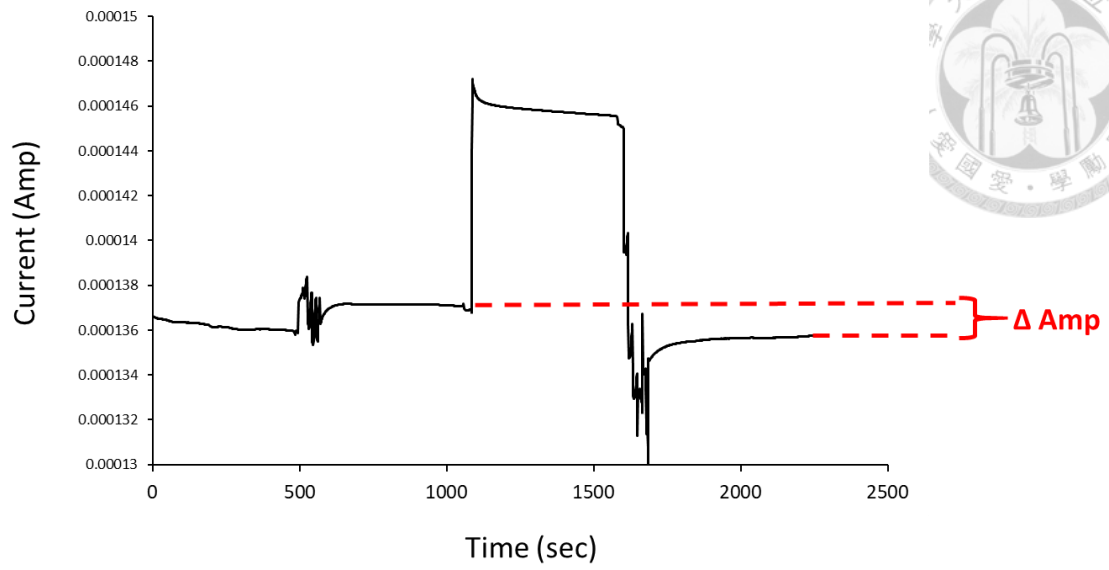
Chip 194, AKI patient No. 31
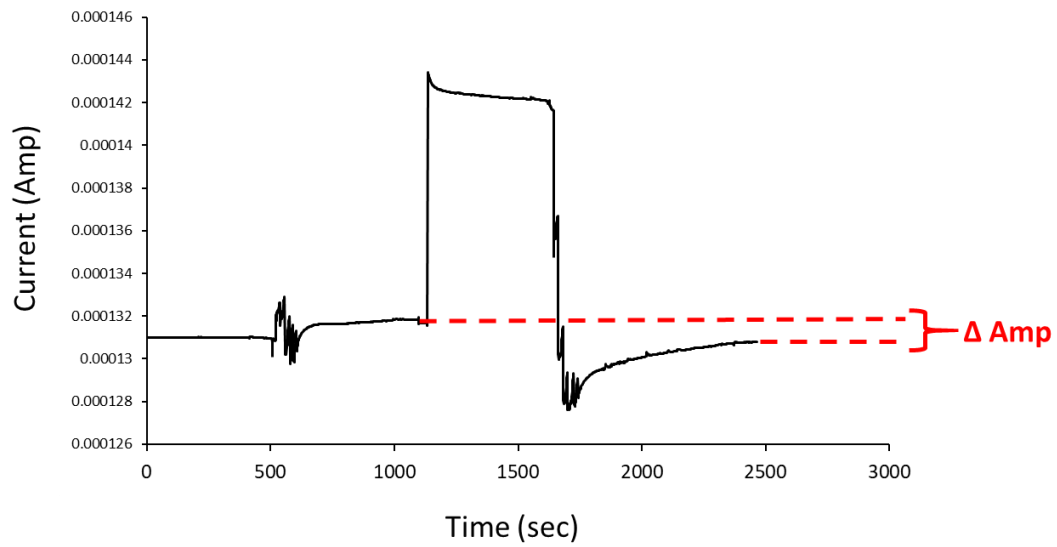
Chip 198, AKI patient No. 31
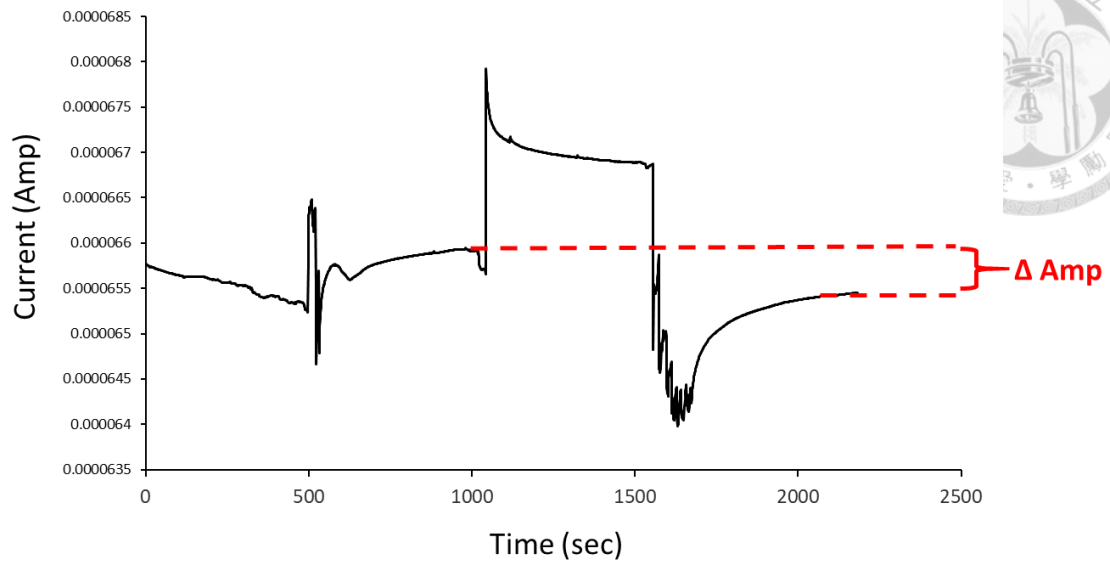
Chip 336, AKI patient No. 33
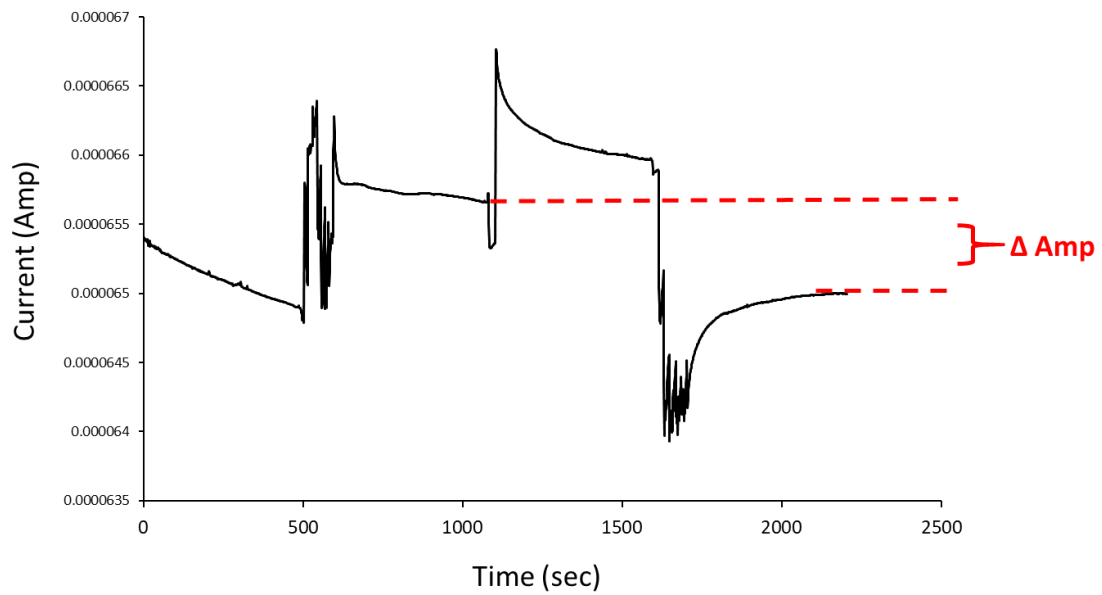
Chip 273, AKI patient No. 33

55
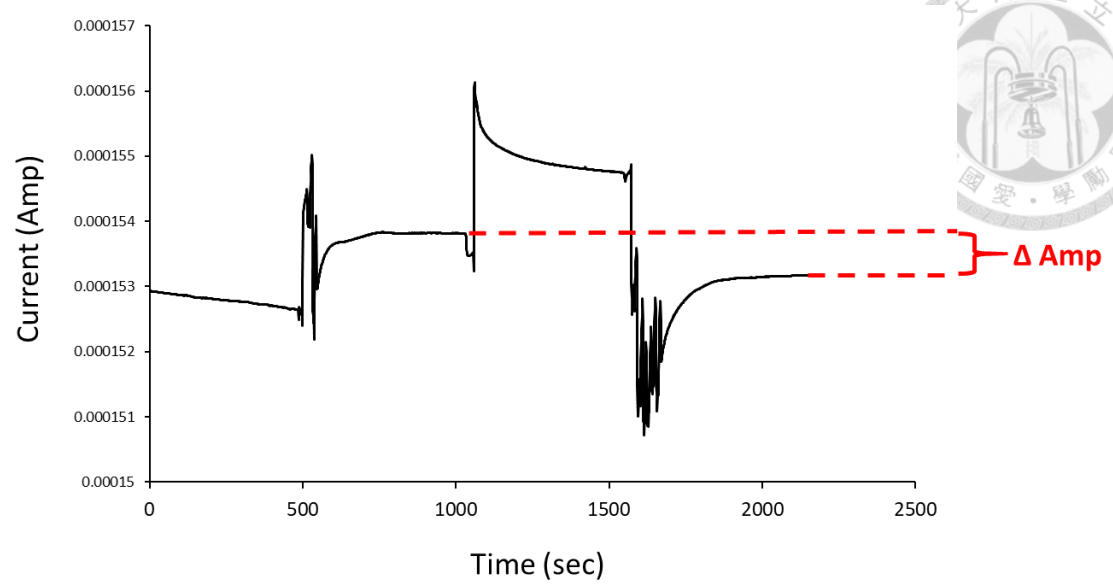
Chip 304, AKI patient No. 33
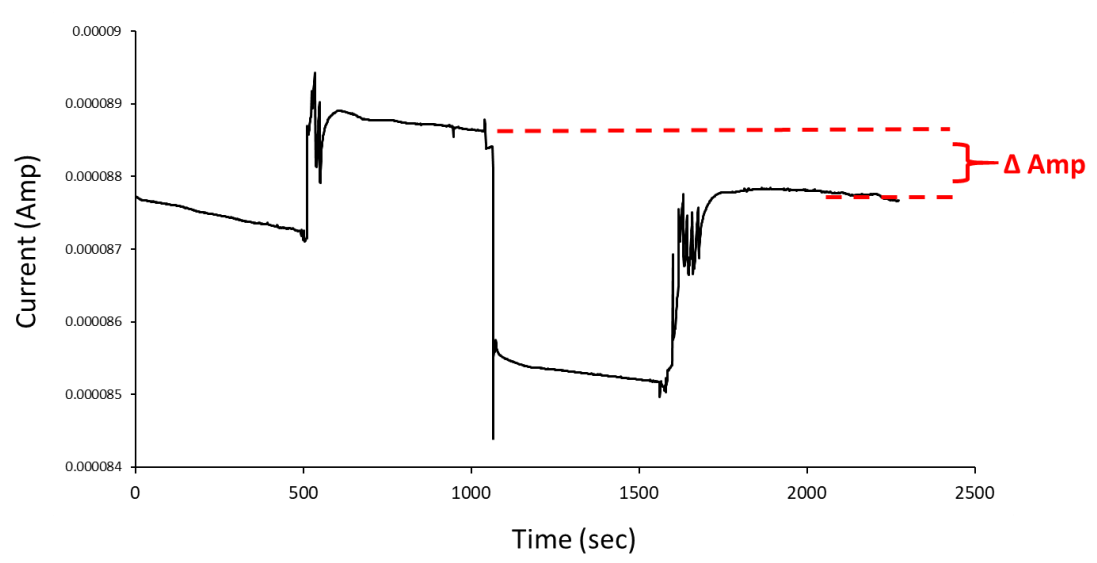
Chip 233, AKI patient No. 27

56
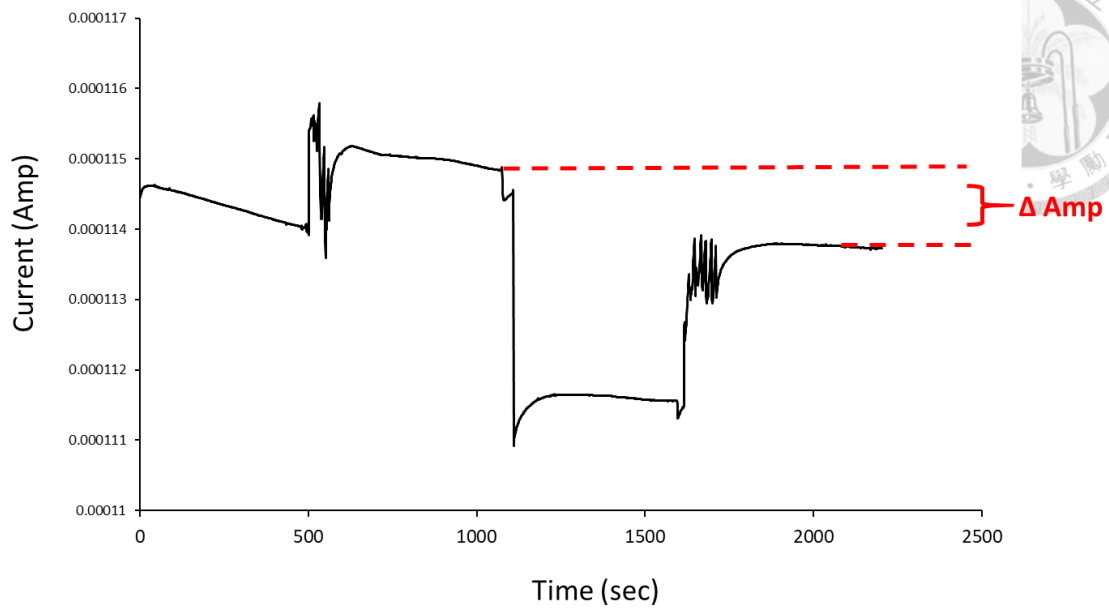
Chip 274, AKI patient No. 27
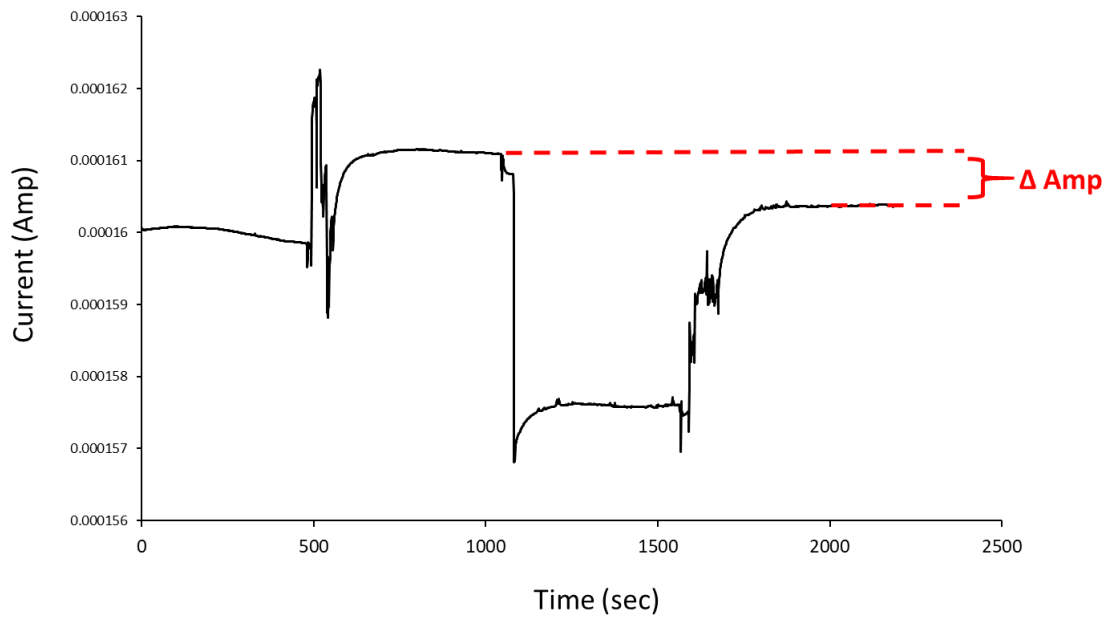
Chip 299, AKI patient No. 27
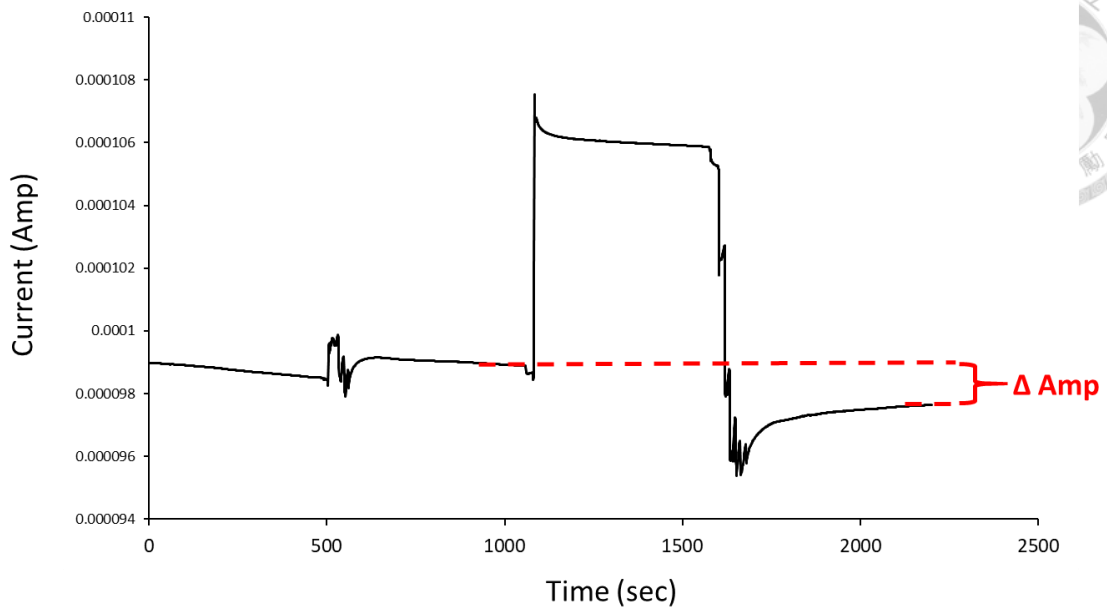
Chip 253, AKI patient No. 34
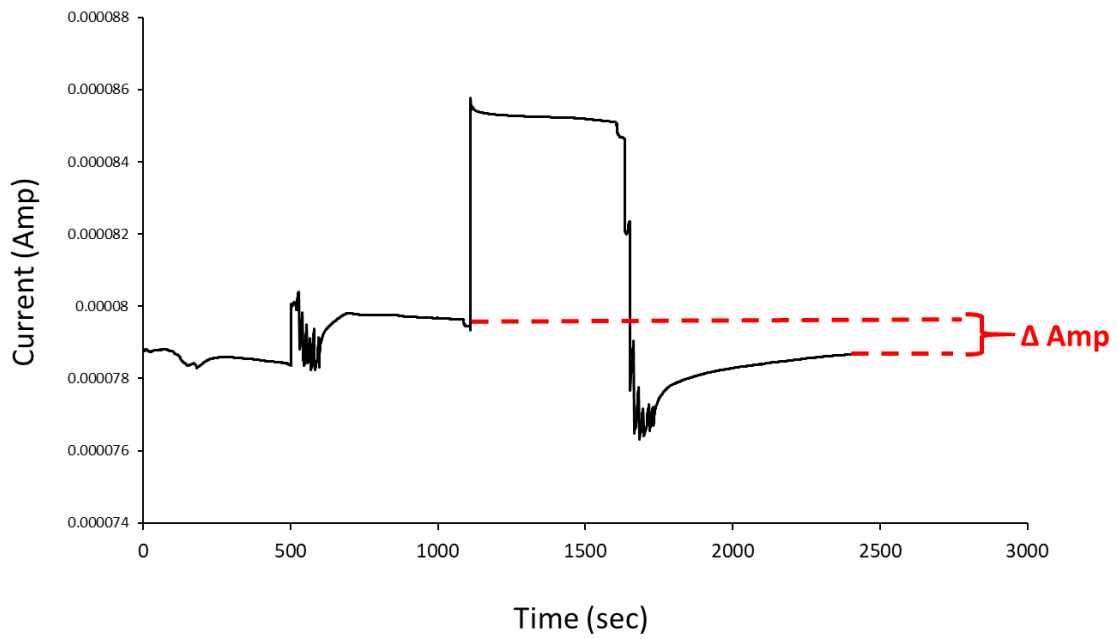
Chip 259, AKI patient No. 34

58
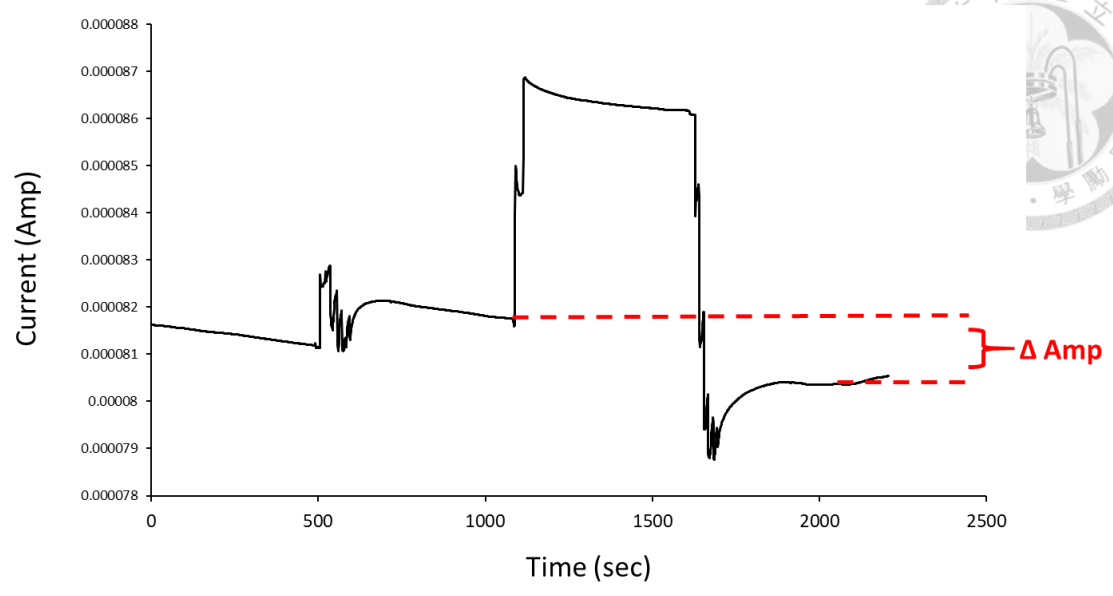
Chip 269, AKI patient No. 34
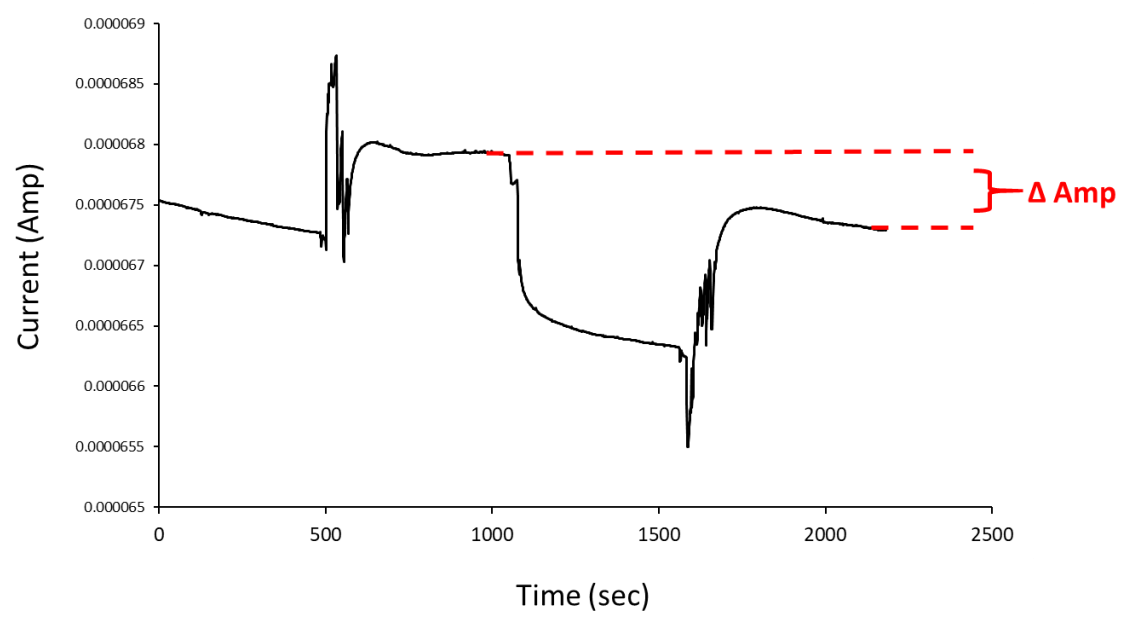
Chip 281, AKI patient No. 45
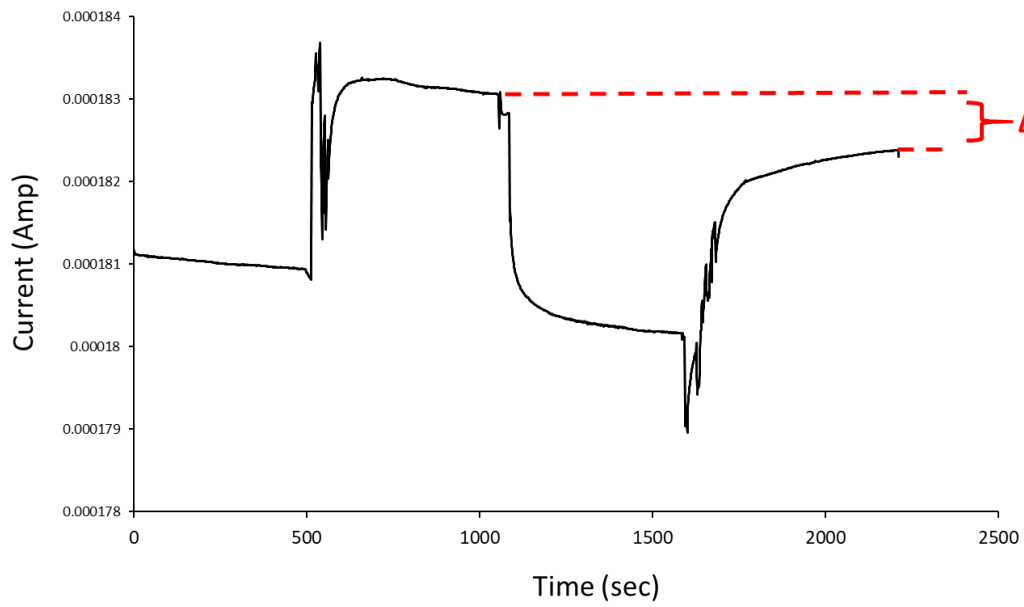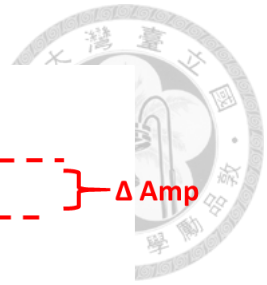
Chip 289, AKI patient No. 45
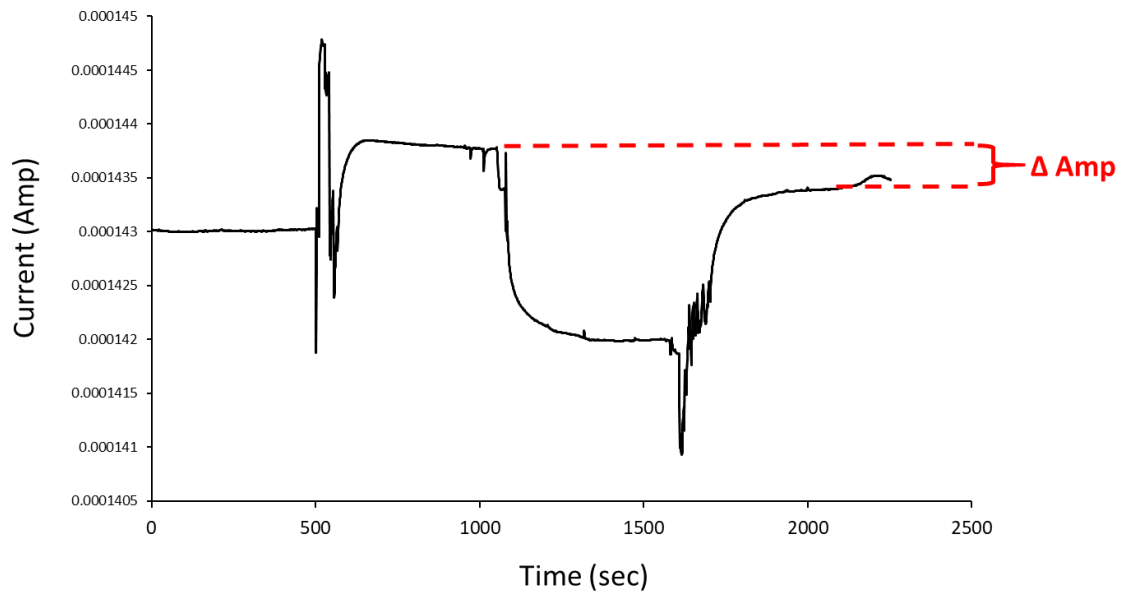
Chip 294, AKI patient No. 45
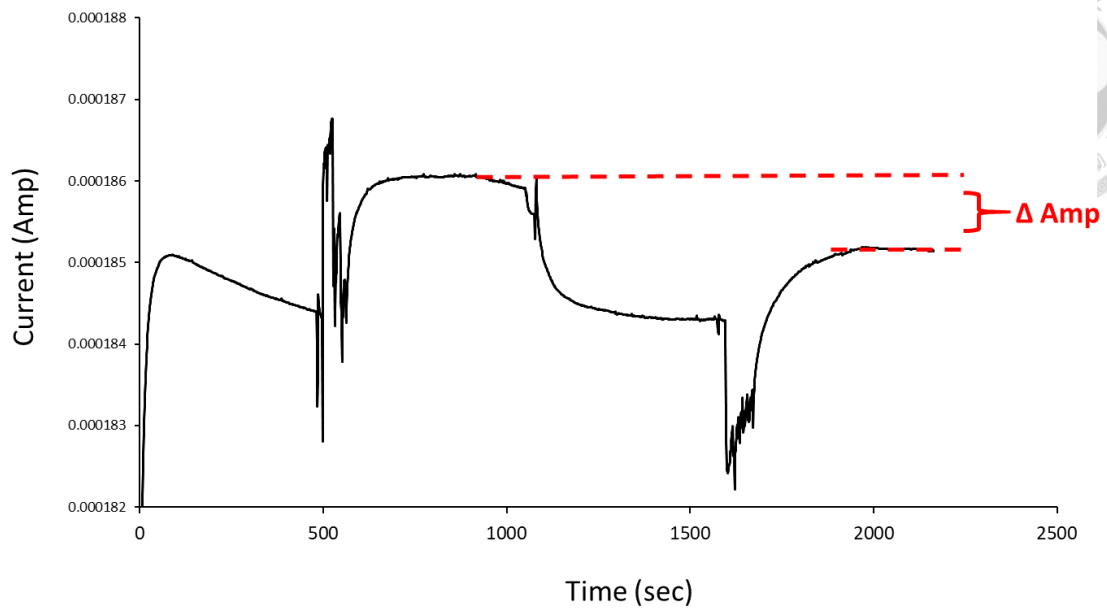
Chip 296, AKI patient No. 44
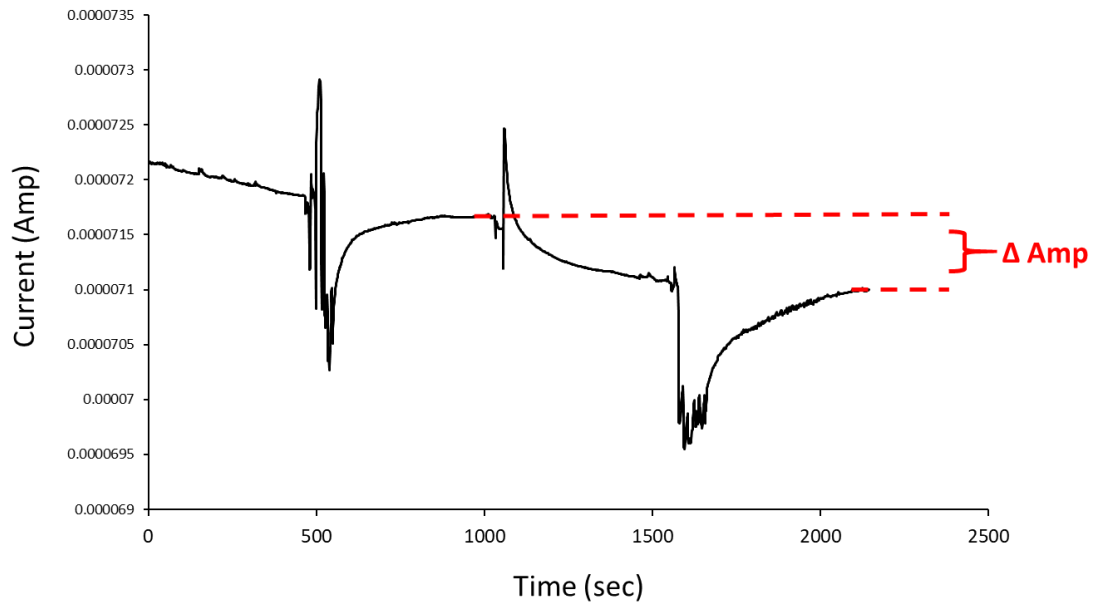
Chip 312, AKI patient No. 44

61
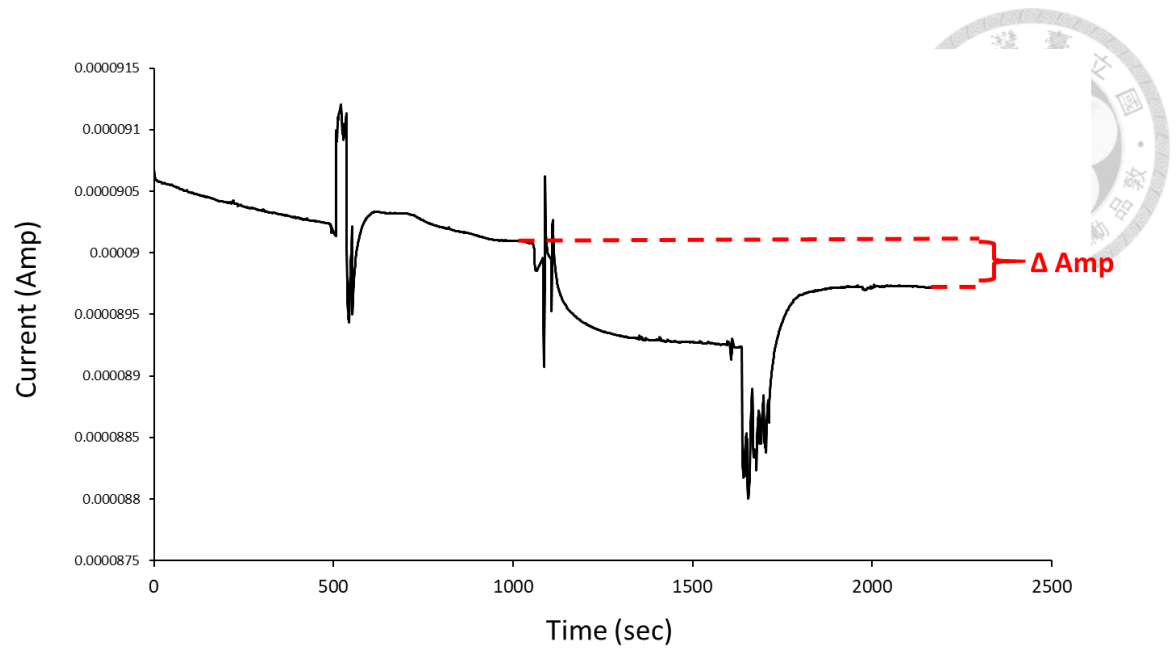
Chip 323, AKI patient No. 44
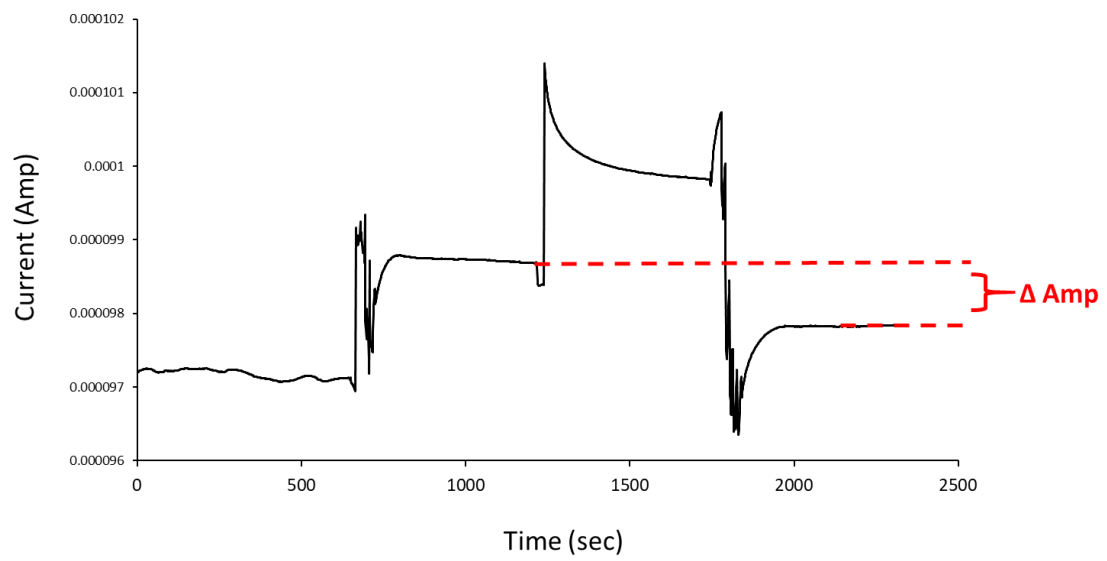
Chip 326, AKI patient No. 168

62
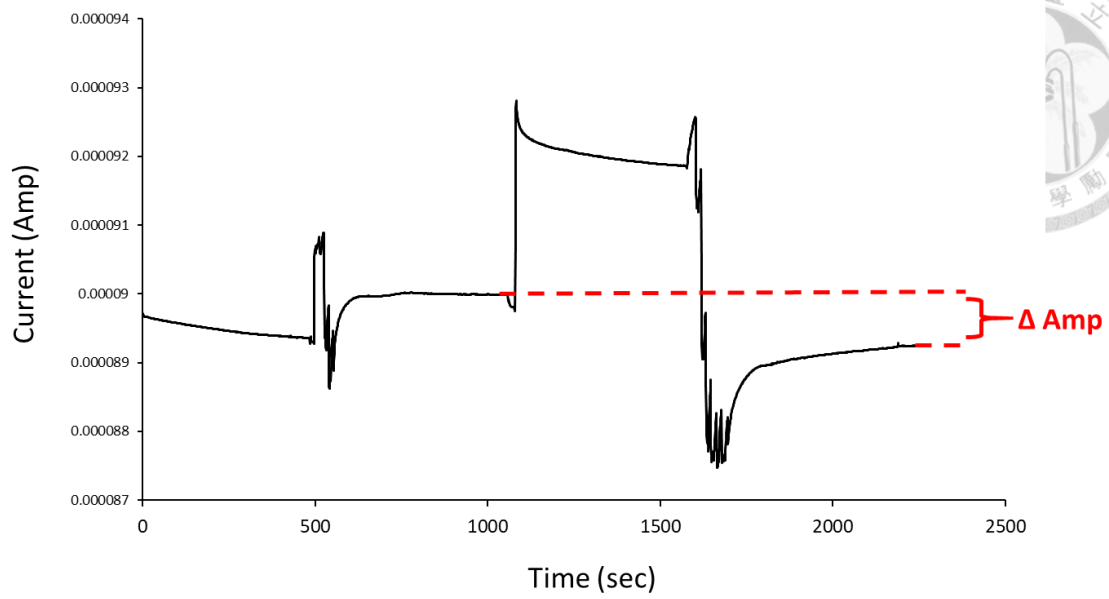
Chip 328, AKI patient No. 168
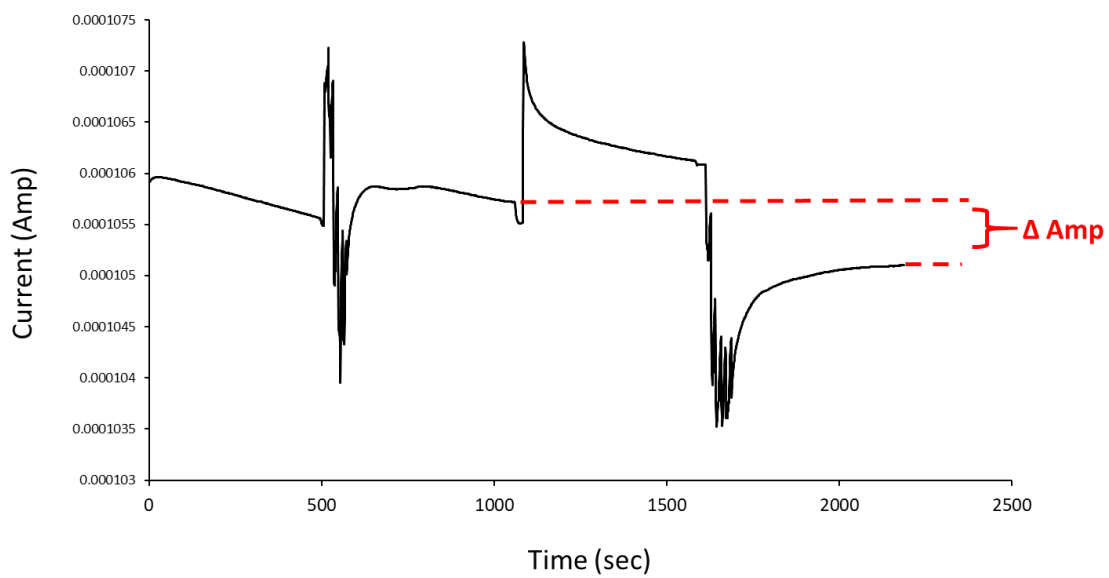
Chip 330, AKI patient No. 168

63
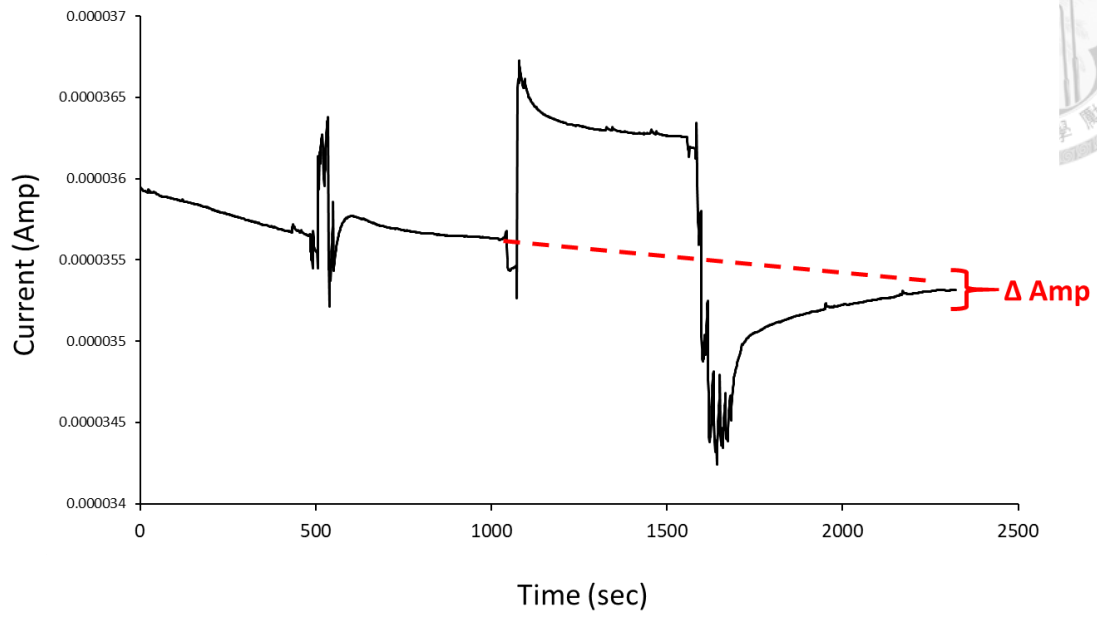
Non-AKI

Chip 337, non-AKI No.1
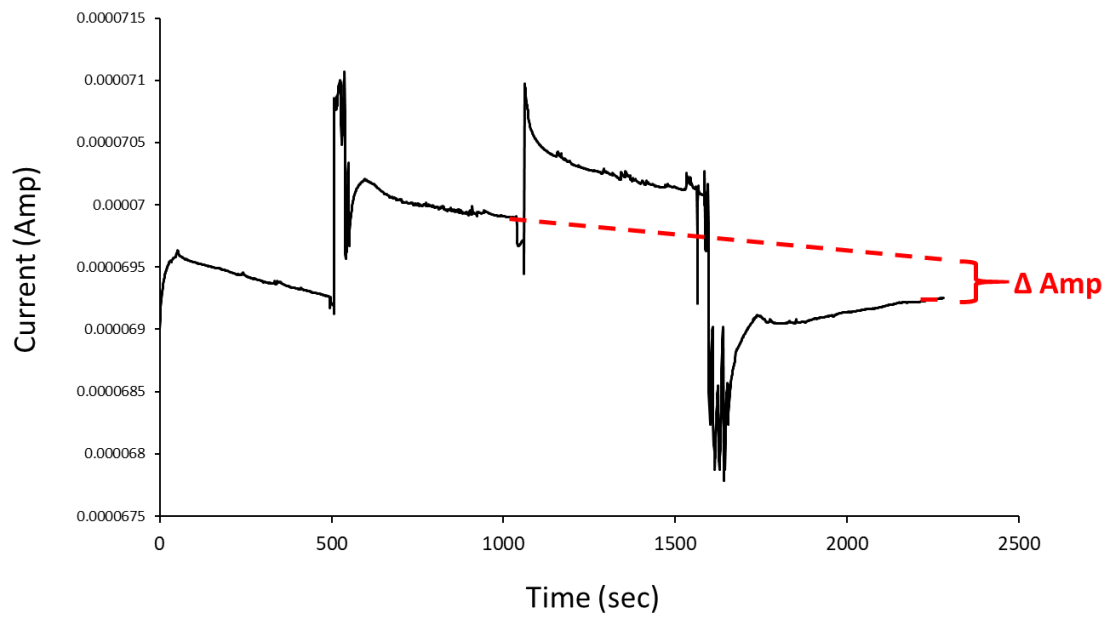
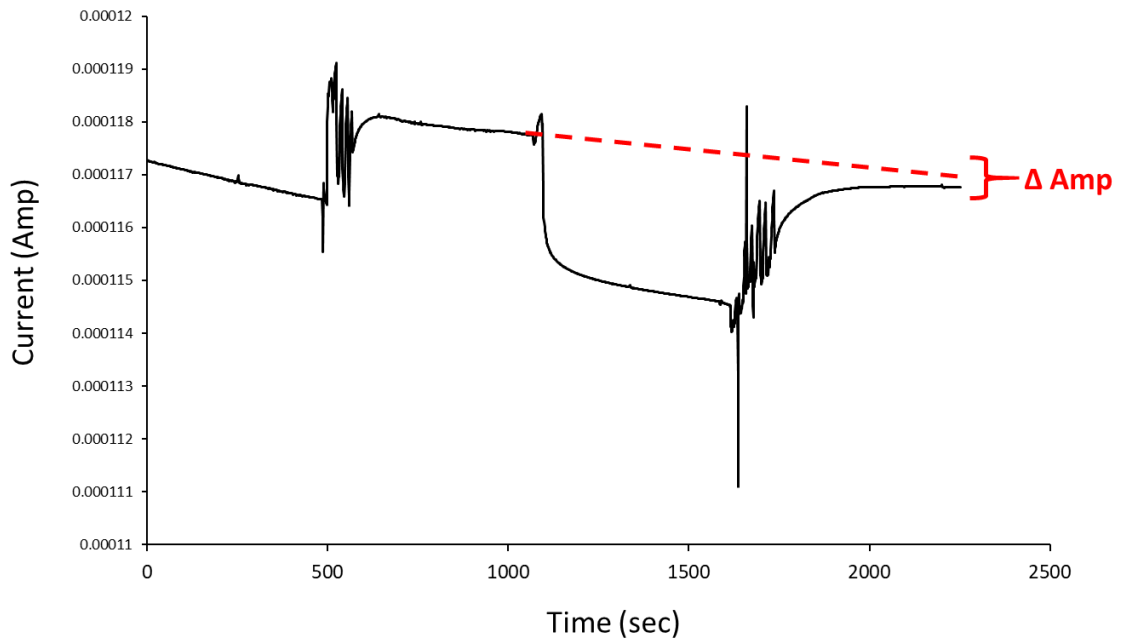Chip 338, non-AKI No.1
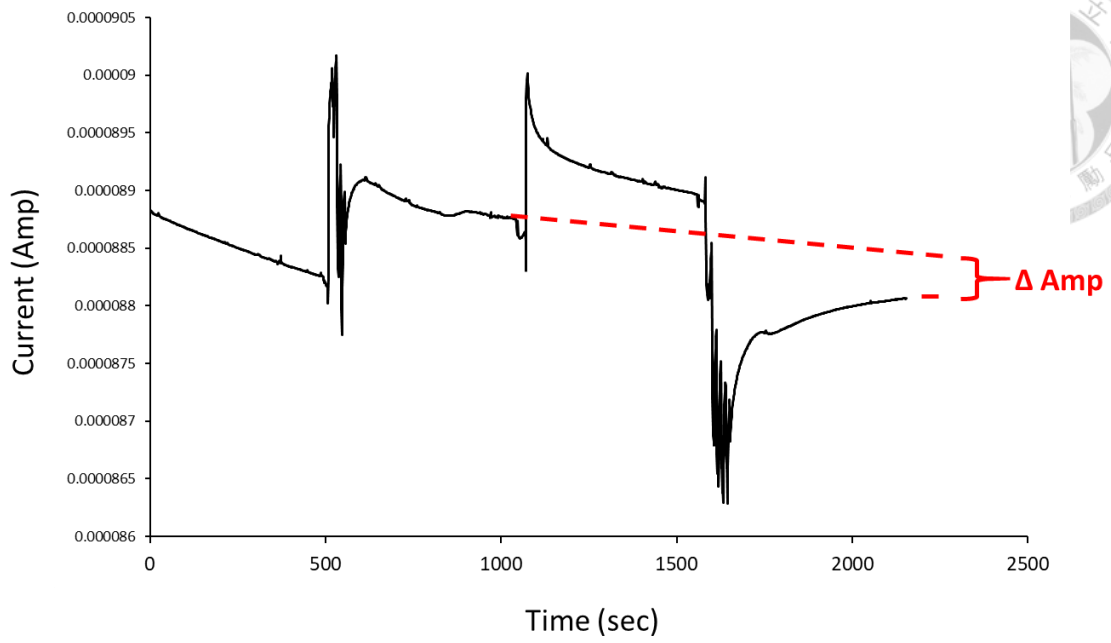
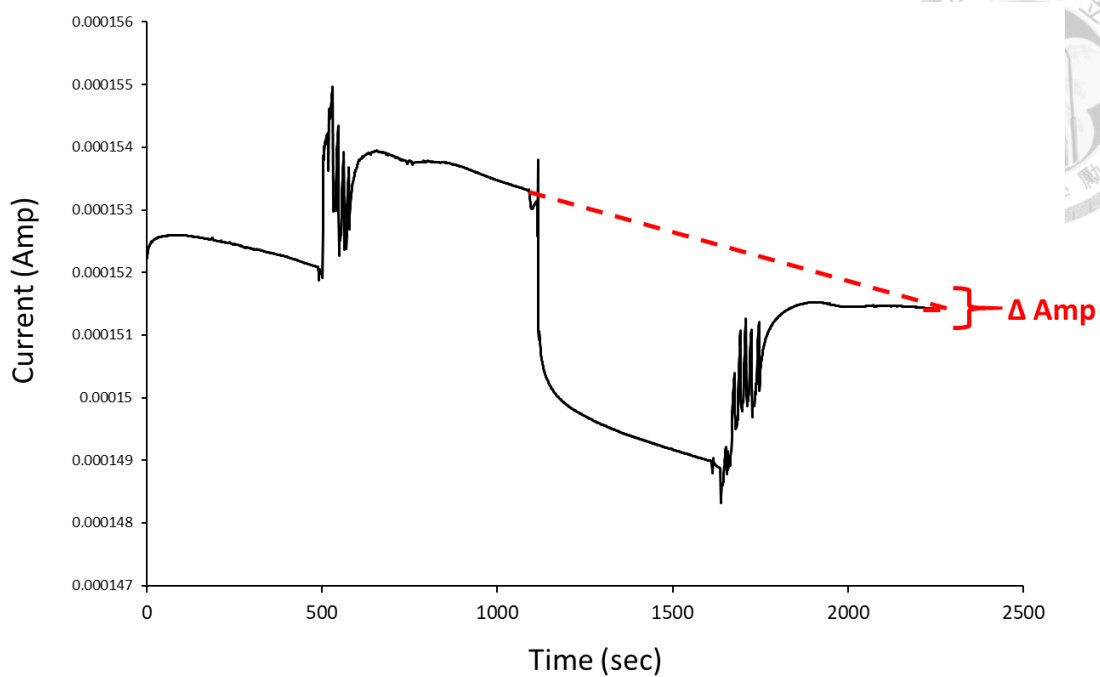Chip 339, non-AKI No.1
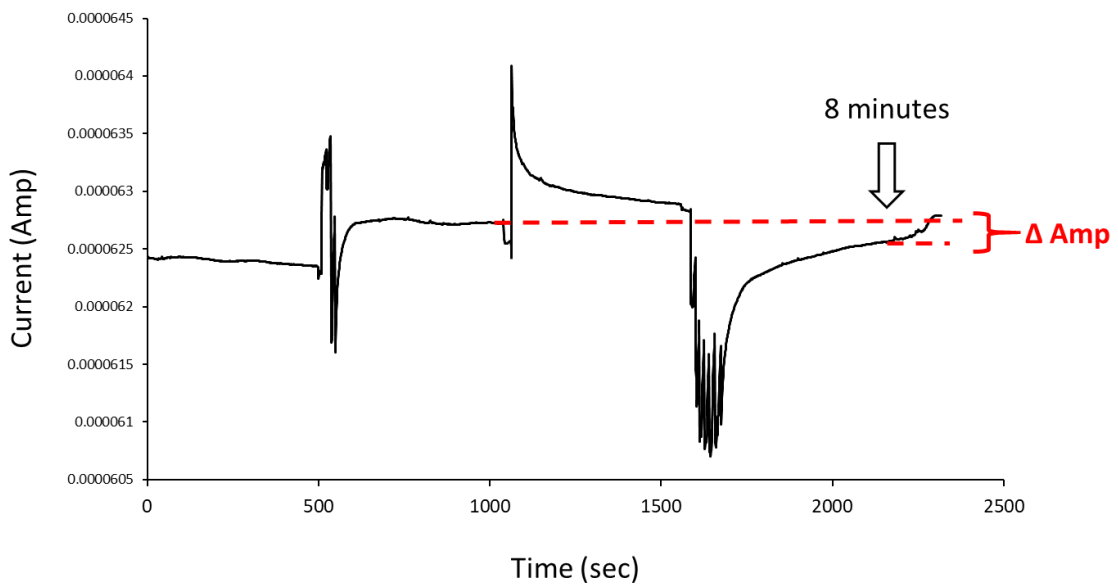
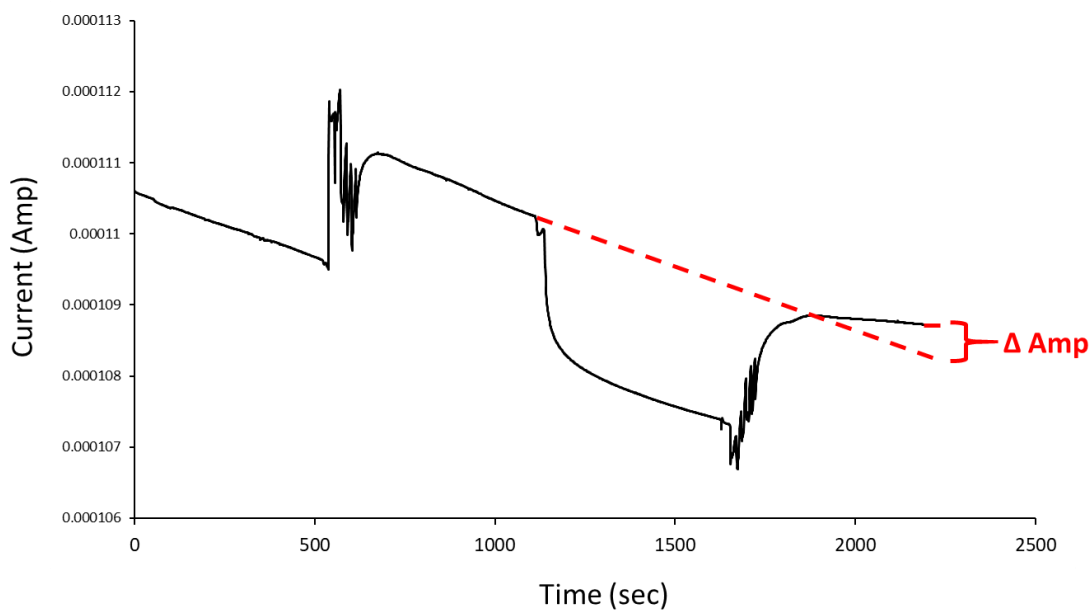Chip 349, non-AKI No.2
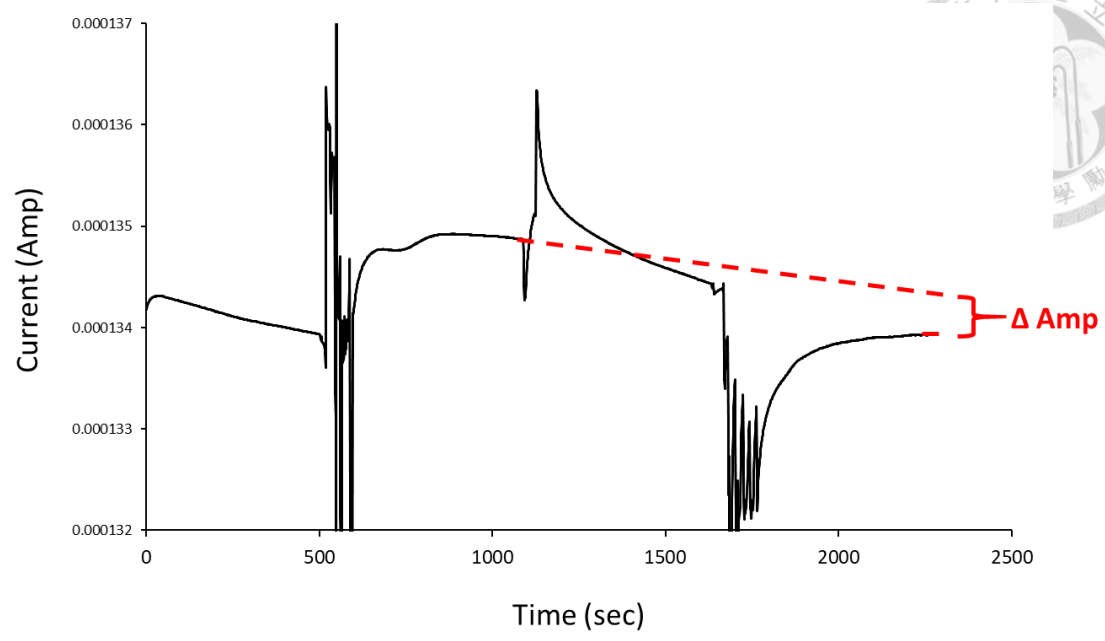
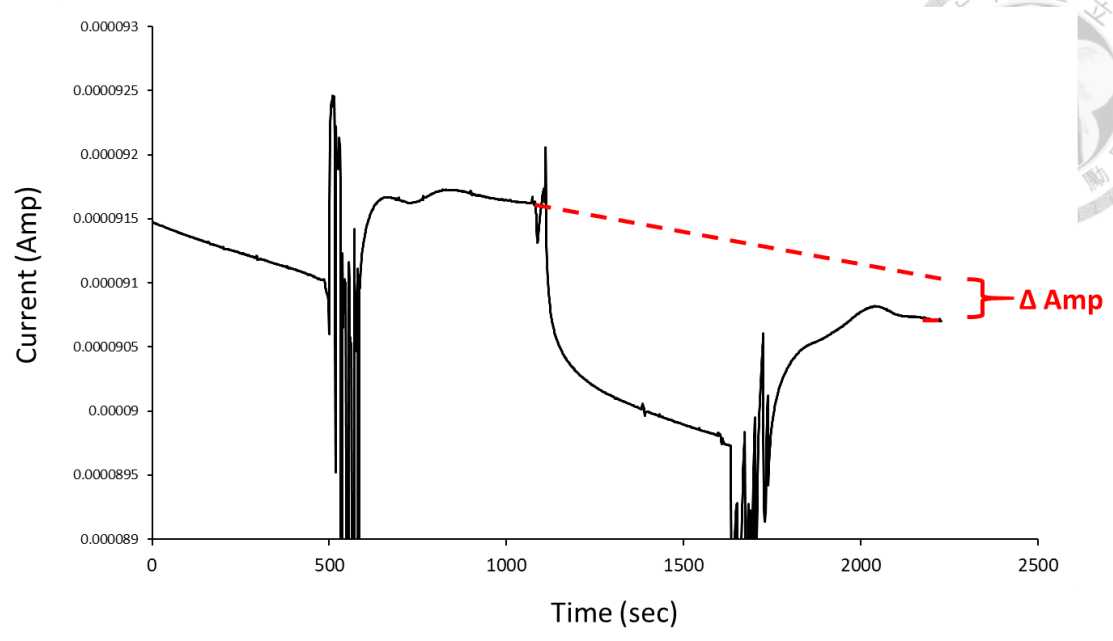Chip 370, non-AKI No.2
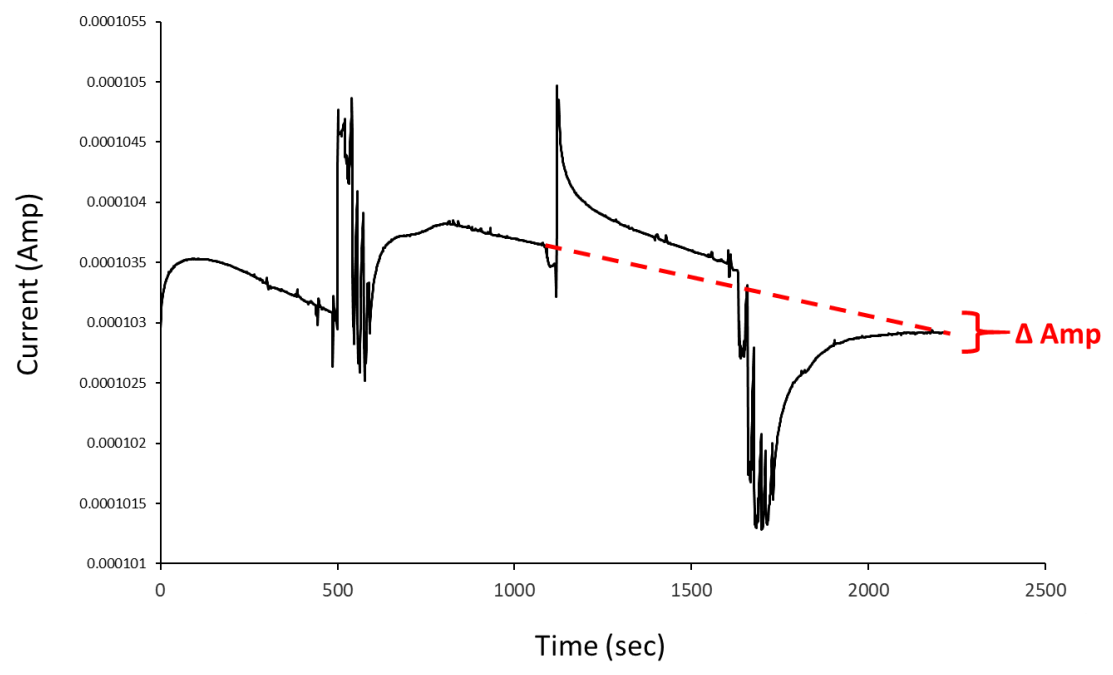
Chip 372, non-AKI No.2
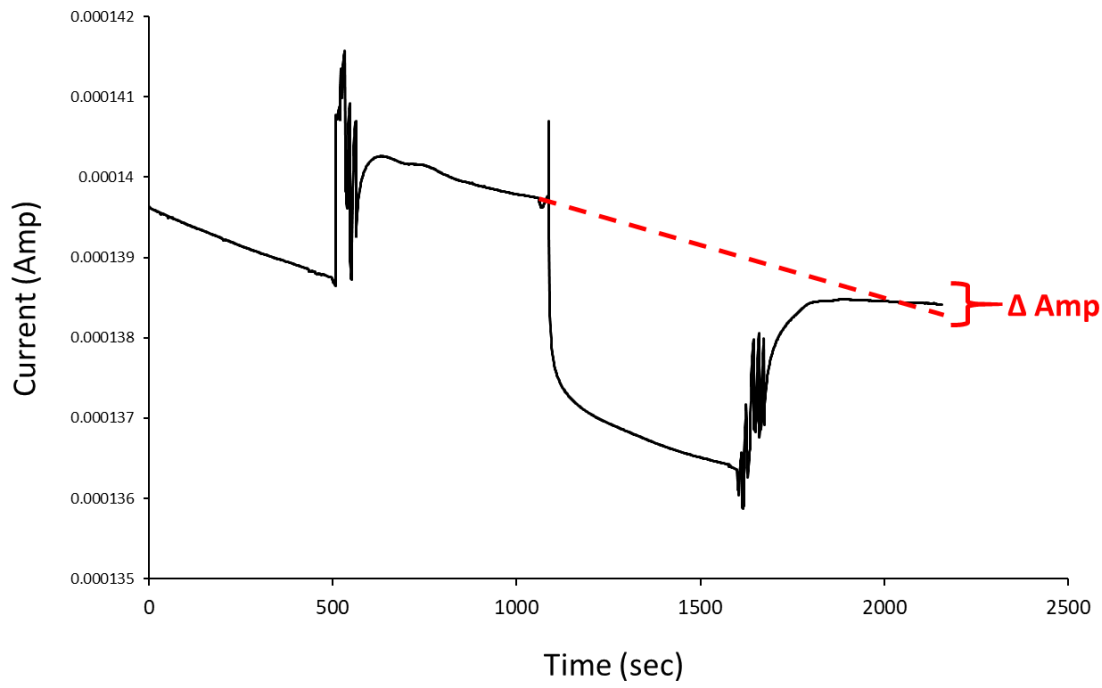
Chip 385, non-AKI No.7

Chip 388, non-AKI No.7
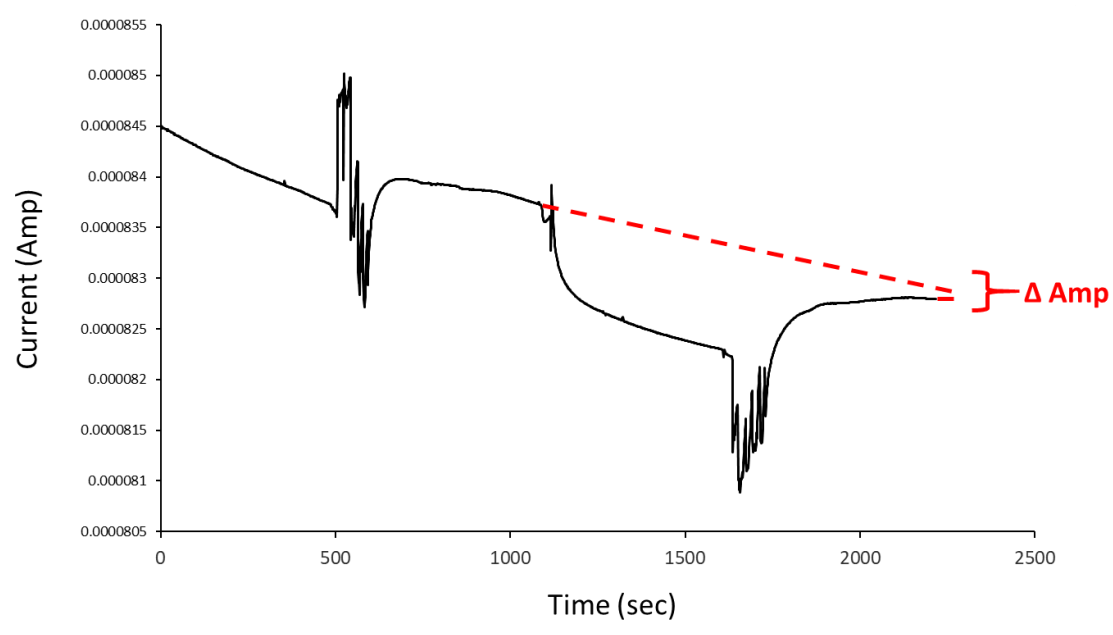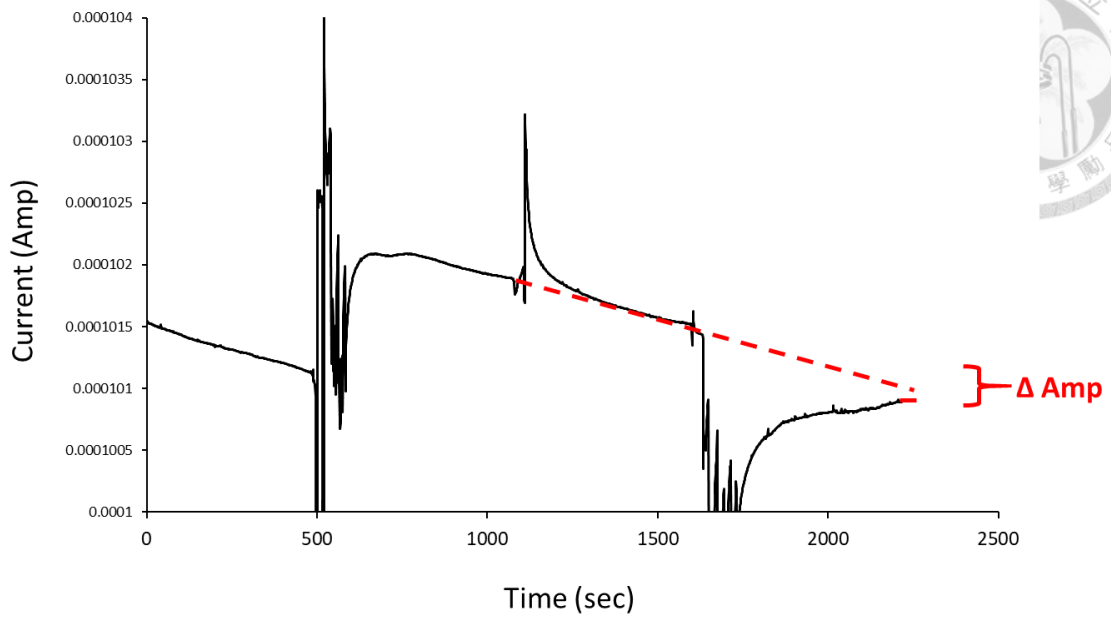
67

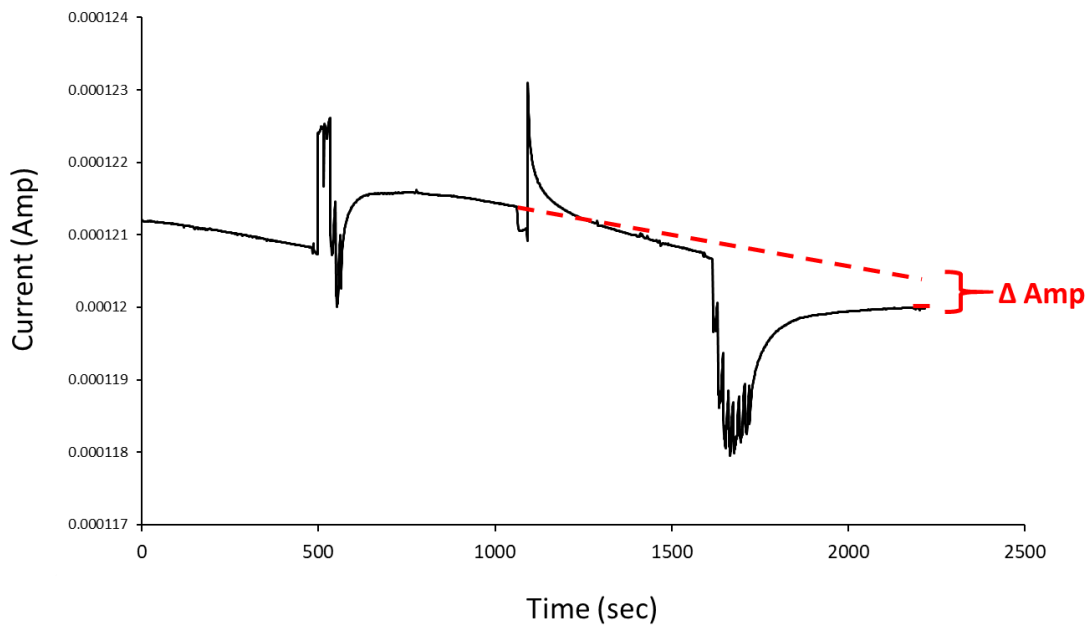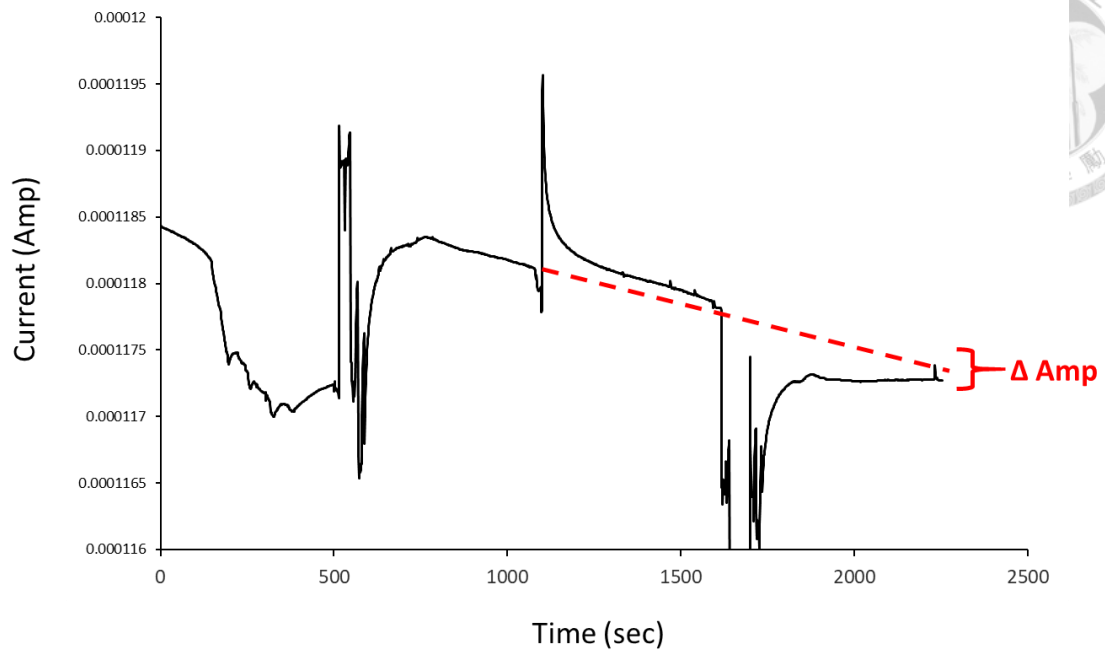Chip 389, non-AKI No.7

Chip 392, non-AKI No.8

Chip 398, non-AKI No.8

Chip 399, non-AKI No.8

69

Chip 401, non-AKI No.3

Chip 414, non-AKI No.3

70

Chip 415, non-AKI No.3

Chips for standard curves

Chip No.	NGAL concentration (ng/mL)	Δ amp
138	1	2.52E-07
140	1	1.12E-07
141	1	1.32E-07
148	1	1.32E-07
151	10	3.12E-07
160	10	3.12E-07
163	10	1.74E-07
105	100	5.54E-07
107	100	4.27E-07
167	100	5.83E-07
87	400	9.56E-07
88	400	1.35E-06
90	400	9.26E-07
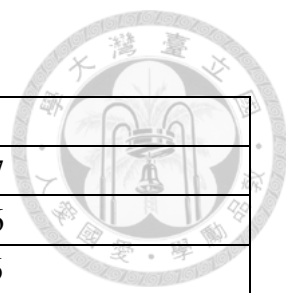
Chips for AKI sample

Chip No.	Patient No.	Δ amp
192	31	8.82E-07
194	31	1.38E-06
198	31	1.11E-06
336	33	4.73E-07
273	33	6.67E-07
304	33	5.2E-07
233	27	9.31E-07
274	27	9.71E-07
299	27	7.24E-07
259	34	8.72E-07
253	34	1.06E-06
269	34	1.06E-06
281	45	5.57E-07
289	45	5.67E-07
294	45	3.96E-07
296	44	6.77E-07
312	44	6.62E-07
323	44	3.23E-07
326	168	7.79E-07
328	168	7.41E-07
330	168	5.24E-07

Chips for non-AKI samples

Chip No.	Sample No.	Δ amp
337	1	5.02E-08
338	1	1.25E-07
339	1	-2E-07
349	2	1.75E-07
370	2	3.85E-08
372	2	-3.4E-07
385	7	-8.2E-08
388	7	-4.4E-07
389	7	-5.3E-08
392	8	-2.8E-07
398	8	1.53E-07
399	8	-1.2E-07
401	3	3.8E-07
414	3	4.77E-07
415	3	9.15E-09